InsP3 Receptor in *Xenopus* Embryos: Expression and Localization during Embryonic Development and Its Possible Roles in Calcium Mobilization during Cell Division Cycle

Akira Muto

Doctoral Thesis
Submitted to the Faculty of Science
Osaka University
1995

Abbreviations:

ATP; adenosine 5'-triphosphate

DAPI; 4,6-diamidino-2-phenylindole

DNA; deoxyribonucleic acid

DTT; DL-dithiothreitol

EDTA; ethylenediaminetetraacetic acid

EGTA; ethylene glycol-bis(β-aminoethyl ether) N,N,N',N'-tetraacetic acid

FITC; fluorescein isothiocyanate

GST; glutathione-S-transferase

$InsP_3$; D-myo-inositol-1,4,5-triphosphate

IPTG isopropyl β-D-thiogalactopyranoside

β-ME; β-mercaptoethanol

PAGE; polyacrylamide gel electrophoresis

PI; phosphatidylinositol

PIPES; piperazine-N,N'-bis[2-ethane-sulfonic acid];1,4-piperazine-diethanesulfonic acid

PMSF; phenylmethylsulfonyl fluoride

RNA; ribonucleic acid

SDS; sodium dodecyl sulfate

Summary

Inositol-1,4,5-trisphosphate($InsP_3$) is known to act as a second messenger in the transmembrane signaling events triggered by such as neurotransmitters, growth factors, and hormones, etc. $InsP_3$ is produced by hydrolysis of phosphatidyl inositol-4,5-bisphosphate and mobilizes free calcium from intracellular stores by opening the $InsP_3$ receptor/Ca^{2+} channel. However, besides transmembrane signaling, the roles of $InsP_3$/calcium signaling linked to endogenous cell cycle regulation has been suggested. To investigate the functions of $InsP_3$/calcium signaling in cell division cycle and embryogenesis, (I) calcium dynamics and the involvement of $InsP_3$ receptors in cell division cycle of *Xenopus* embryos were examined, and (II) the expression and localization of $InsP_3$ receptors through development were studied.

(I) The changes of intracellular free calcium in early cleavage-stage *Xenopus* embryos were examined using fluorescent calcium indicator dye, Calcium Green-1. Free calcium rises were observed at the cleavage furrow in each cleavage. The rise of free calcium propagated along the cleavage furrow as calcium waves. In the absence of extracellular calcium, the calcium waves were observed to accompany the cleavage furrow extension. After fertilization the intracellular free calcium was observed to oscillate with the periodicity equal to that of the cell cycle. Both the rise of free calcium at the cleavage furrow and the periodic free calcium oscillation were inhibited in embryos injected with an $InsP_3$ receptor antagonist, heparin. These results implicate that $InsP_3$/calcium signaling is activated endogenously during cell division cycle and has some roles in cell cycle regulation.

(II) The localization of $InsP_3$ receptor through development were examined with a specific antibody against *Xenopus* $InsP_3$ receptor. The antibody was raised on the basis of primary structure of *Xenopus* $InsP_3$ receptor whose cDNAs were cloned and sequenced previously (Muto,1992(Master Thesis, Osaka Univ.), Kume et al., 1993). $InsP_3$ receptors were present in the

cytoplasm of the entire cell with highly polarized distribution to animal hemisphere in early-stage embryos and were also enriched in the perinuclear region. In the early embryonic development, $InsP_3$ receptors were immunolocalized to ectoderm in gastrula embryos, to ectoderm, neural tube, somites and notochord in neurula embryos.

Introduction

Embryogenesis has two aspects: one is cell division which establish multicellularity and the other is the interaction between divided cells. Cell signalling is thought to play important roles both in cell cycle regulation and embryonic induction. Inositol 1,4,5-trisphosphate($InsP_3$) is well known to act as a second messenger to transduce extracelluar signals through the plasma membrane, which causes free calcium mobilization from intracellular calcium stores (Berridge, 1993). In addition to the roles as a second messenger, within a cell, $InsP_3$/calcium signaling has been suggested to have some roles in cell cycle regulation. The changes of $InsP_3$ mass and intracellular free calcium during embryonic cell cycle of sea urchin were observed (Ciapa et al., 1994). So the $InsP_3$/calcium signalling system can have some roles in both cell division cycle and embryonic development where the cell-cell interaction has critical roles.

Calcium ions are thought to participate in the regulation of several aspects of cell division (Hepler 1994). Calcium oscillation during cell division are observed in *Xenopus* embryos (Grandin and Charbonnneau, 1991, Kubota et al., 1993). Intracellular calcium transients are observed at various stages during cell division such as pronuclear migration and fusion, nuclear membrane brake down, anaphase onset and cytokinesis in sea urchin embryos (Poenie et al., 1985, Ciapa et al.,1994) , just before nuclear envelope break down in mouse embryo (Tombes et al., 1992) and at cytokinesis of medaka fish embryos (Fluck et al., 1991). Chelating the intracellular calcium

causes retardation of cell division cycle (Snow and Nuccitelli, 1993). Furthermore, there has been reported that phosphatidyl inositol (PI) turnover are involved in cell cycle progression (Han et al., 1992, Stith et al., 1993) and are coupled to the calcium transients (Ciapa et al., 1994).

Besides the cell cycle progression, there are several lines of evidence which suggest the involvement of PI turnover in embryonic development. Lithium is known to perturb PI turnover and has an teratogenic effect on amphibian development (Busa, 1988, Berridge et al., 1989). In early stage of amphibian development, bath application of lithium chloride can make exaggerate head or dorso-anterior structures and when injected into ventralized embryos by UV irradiation it can respecify the dorso-anterior structures (Kao et al., 1986). Inositol or diacylglycerol analog can rescue the effect of lithium on embryonic axis formation (Busa and Gimlich, 1989).

InsP3 receptor of *Xenopus* oocytes was characterized (Parys et al.,1992) and its cDNAs has been cloned (Kume et al.,1993). The participation of $InsP_3$ receptors in the initiation and propagation of calcium waves at fertilization has been established in many species such as sea urchin (Galione et al., 1993, Lee et al., 1993), hamster (Miyazaki et al., 1992) as well as *Xenopus* (Nuccitelli et al., 1993). However there are little evidence which show the involvement of $InsP_3$ receptor-mediated calcium mobilization in cell cycle regulation.

In the present study, the roles of $InsP_3$ receptor were examined in two aspects: in cell division cycle by calcium imaging technique and in embryonic development by immunocytochemical study.

Results

Measurement of Free Calcium Changes with Calcium Green-1

In order to make sure that heparin, which was used as an $InsP_3$ receptor blocker in the present study, did not affect the fluorescence of Calcium Green-1, the fluorescence of the dye at various concentration of free calcium with or without heparin was measured. As shown in Figure 1, neither heparin nor De-N-sulfated heparin, which was used in control experiments, affected the Calcium Green-1 fluorescence.

As *Xenopus* eggs are extraordinary huge (1.1-1.3 mm in diameter), the time needed for the injected dye to diffuse throughout the egg was examined. Fully grown *Xenopus* oocytes which are naturally arrested at prophase of meiosis I and whose intracellular calcium concentration is supposed to be constant, were used for the estimation. *Xenopus* oocytes were injected with Calcium Green-1 at four points in the equatorial region near the animal pole. The injected oocytes were placed under an inverted microscope and the fluorescence from the vegetal side was monitored with a laser confocal system, Bio-Rad MRC-500. The intensity of the fluorescence of the dye increased even 3 hours after dye injection suggesting that it takes more than 3 hours for the dye to diffuse throughout the entire oocytes at 24°C (Figure 2). Considering the above results obtained in the oocytes, the gradual increase of the fluorescence of embryos observed below is possibly due to the diffusion of the dye but not reflecting the increase of intracellular calcium concentration.

Free Calcium Rises at Cleavage Furrow

To detect the changes of intracellular free calcium during cell division cycle, *Xenopus* eggs were fertilized *in vitro*, injected with calcium indicator dye, Calcium Green-1 at 1-cell stage and placed at 17°C for about 1 hour to allow the dye to diffuse. Since the animal hemispheres of *Xenopus* eggs are

pigmented, and the animal poles of fertilized eggs are oriented upward, the eggs were observed from the vegetal side using an inverted microscope. In order to maximize the detectable fluorescence, the confocal aperture was set to fully open condition and the focal plane was determined so that the most uniform intensity over the images could be obtained. The first and the second cleavage of *Xenopus* eggs are initiated at the animal pole and the cleavage furrows progressed toward the vegetal pole. The measurement was started when the first cleavage furrow progressed to the equatorial region. The timing of the start of measurement was designated as time 0' in the present study. Rises of free calcium at cleavage sites were observed. A typical example of the calcium wave pattern in an embryo which grew up to tadpole stage after the measurement is shown in Figure 3a. After the completion of the first cleavage (at 16' , Figure 3a), free calcium rises were observed at the first cleavage furrow (at 30'-36', Figure 3a). The newly formed two blastomeres were separated from each other by a broad and obvious groove (at 28', Figure 3a), then the groove become somewhat obliterated (at 38' Figure 3a) after the calcium waves had occurred. So the cleavage furrow seemed to be 'zipped' after the free calcium waves had passed (compare the images of cleavage furrows at 28' and 38', Figure 3a). When the second cleavage was progressing around equatorial region, calcium transients often occurred at the first cleavage furrow again (see the images at 48' and 50', Figure 3a). The second cleavage furrow was also accompanied by calcium waves (60'-66'). The rises of free calcium at the cleavage sites were observed in all succeeding cleavages at least until blastula. The averaged fluorescence in the ROI (region of interest) of the same embryo as Figure 3a was plotted in Figure 3b. The rise at the first cleavage furrow appeared as a sharp peak at 32' (Green). The rise at second cleavage furrow also appeared as a peak at 58' (Red). The maximum changes of fluorescence was about 1.3-fold compared to the value just before the transient. Note that the fluorescence in

both ROIs showed a peak at about 20' which was not associated with any rises at the cleavage furrows. These peaks correspond to the first peak of free calcium oscillation described below (see below for detail). Although the free calcium rises at the cleavage furrow was consistently observed in all experiments, the spatio-temporal pattern of calcium transients at the cleavage furrows somewhat varied from egg to egg. In some cases the waves were observed to occur from the animal side of the embryo and propagated towards the vegetal pole. In other cases, the wave initiated at around the vegetal pole, and propagated around there. The rise of free calcium at the tip of the elongating furrow was also observed in some cases (see discussion).

The Calcium Waves Are Independent of Extracellular Calcium

To determine whether the calcium ion was released from intracellular calcium stores, the measurement was done in distilled water containing EGTA. When grown in distilled water or in the presence of more than 10μM EGTA, the contact of blastomeres were loosen and the embryos often died after several times of cell division cycle. However, the calcium waves were always observed following the cleavage furrow formation in the presence of EGTA, at least in the first cell division. A typical example is shown in Figure 4 in which the egg was placed in 20μM EGTA. The calcium waves were observed to accompany the first cleavage furrow (10'-13.5', Figure 4a). They propagated from the animal pole side in two direction and combined together when they reached the vegetal pole (at 13.5', Figure 4a). Then it ceased (21'-23', Figure 4a) and the waves appeared once more at the first cleavage furrow (23.5', seven o'clock direction, Figure 4a). At 25.5' the second cleavage furrow is coming to the equatorial region. The maximum changes of dye intensity was 1.6-fold to the value just before the transient. In another example it was 1.45-fold.

The velocity of the wave shown in Figure 4a was calculated, assuming that the calcium wave had progressed in the cortical region near the surface of the egg. The length of the arc L, which the wave front had passed along is calculated as L=R x arccos(1-D/R), where R=550 μm (radius of the egg), D is the distance the wave front had passed on the images. L was plotted as a function of time in Figure 4b. The velocity was calculated as 2.8 μm/sec. The above results indicated that there are mechanisms by which calcium waves are formed along the cleavage furrows independent of extracellular calcium.

The Calcium Waves at the First Cleavage Furrow Are Blocked by Heparin

To examine the mechanism of the calcium wave formation at the cleavage furrow, heparin was used as an $InsP_3$ receptor blocker. Twenty nl of 2mg/ml heparin (Approx. MW=3500, Sigma) was co-injected with the dye into fertilized eggs. The estimated final concentration of the injected heparin in the cytoplasm was about 90μg/ml assuming that the volume of the cytoplasm as 450nl (Nuccitelli et al., 1993, Paine, 1984). The localized rise of dye intensity at the cleavage furrow were significantly inhibited in heparin-injected eggs (Figure 5). In control embryo injected with the same amount of De-N-sulfated heparin showed rises of dye intensity between the completion of the first cleavage and the second cleavage (13'-23', Figure 5). The free calcium rise at the first cleavage in heparin-injected embryo was inhibited. Note that at 48' the second cleavage furrow is progressing toward the equator in heparin-injected embryo. The second cleavage did not complete normally and this embryo failed to survive. Similar results were obtained in five out of six embryos observed. Both the timing of the onset of the first cleavage furrow and the furrow formation was retarded in heparin-injected embryos and the cell divisions thereafter were inhibited or greatly retarded.

The averaged fluorescence in ROI of both images were plotted to show that there was no free calcium rise at the first cleavage furrow of the heparin injected egg during the measurement (Figure 5b).

As shown in Figure 3, 'zipping' of cleavage furrow occurred during free calcium rises in control embryo but not in heparin-injected embryo (compare the images of cleavage furrow at 8' and 28' in Figure 5).

Intracellular Free Calcium Oscillates with the Period of Cell Division Cycle

In addition to the local calcium rise at the cleavage furrow, free calcium changes over the entire embryo at early cleavage stages were monitored. The averaged intensity of the fluorescence over the entire embryo was plotted. A typical result of an embryo is shown in Figure 6. The period of oscillation was 24.8 min. at 26°C. The fluorescent images of the embryo at each peak are shown in the figure. The periodicity of the oscillation is equal to that of the cell division cycle, and each peak corresponded approximately to the completion of each cleavage. Note that the image shown here are a vegetal view, therefore the third cleavage which occurs in the horizontal plane is out of view. These results confirmed the detection of free calcium oscillation using calcium micro electrodes (Grandin and Charbonneau, 1991) and aequorin luminescence (Kubota et al. 1993). The free calcium waves at the cleavage furrow described above (Figure 3) and the free calcium rise in oscillation were distinct phenomena. Note that in Figure 6, there are no free calcium rises at the cleavage furrow at the timing of each peak. It was confirmed by the fact that the free calcium oscillation did occurred in cleavage-arrested embryos (see below).

Therefore, two patterns of free calcium changes in *Xenopus* embryos were observed: one is oscillatory and the other is localized waves at the cleavage furrows.

The Free Calcium Oscillation is Independent of Cytokinesis

Kubota et al. (1993) previously reported that the oscillation of intracellular free calcium occurred in colchicine-injected, cleavage-arrested *Xenopus* embryos. This observation was confirmed in the present study using Calcium Green-1. Twenty nl of 0.5mg/ml colchicine was co-injected with the dye into fertilized eggs, which caused the complete inhibition of the cell division. As shown in Figure 7, the intensity of the fluorescence of colchicine-injected embryos oscillated with the period of 40.1+/-3.3 min. (mean +/-SD, n=7) at 24°C. It was comparable with the period of the control embryos (33.8+/-0.85 min. (mean +/-SD, n=3) which was injected with dye alone.

The Oscillation is Independent of Extracellular Calcium and Inhibited by Heparin

To examine the source of the free calcium, the measurements were carried out in distilled water containing 50μM EGTA instead of Steinberg's solution. Since cleaving *Xenopus* embryos died soon in the absence of extracellular ions, cleavage-arrested embryos were used to monitor the free calcium oscillation. Fertilized eggs were injected with 0.5 mg/ml colchicine and 0.5mM dye, and monitored in 50μM EGTA. As shown in Figure 8, the oscillation of colchicine-injected eggs were still observed in the absence of the extracellular calcium. The period of the cycle was 38.0+/-0.77 min. (mean +/-SD, n=9) at 25°C. This value was similar to that obtained from embryos monitored in Steinberg's solution. This indicates that the oscillation is independent of extracellular calcium and that the free calcium was mobilized from the intracellular calcium stores.

To examine the involvement of $InsP_3$ receptors in mobilization of free calcium in oscillation observed above, heparin was used as an $InsP_3$ receptor antagonist. Twenty nl of 2 mg/ml Heparin (estimated final concentration as

90 mg/ml), 0.5 mg/ml colchicine and 0.5 mM Calcium Green-1 were co-injected after fertilization. The oscillation in the heparin-injected embryos was significantly inhibited or greatly retarded (n=9) compared to the control embryos which were injected with equal amount of De-N-sulfated heparin (the period of oscillation: 38.9+/-5.0 min. (mean +/-SD), n=6). The period of cell cycle of embryos injected with dye alone was 24.3+/-1.4 min. (mean +/-SD, n=3, R.T.=25°C.) A typical result was shown in Figure 9. These results suggests that free calcium oscillation during cleavage stage of *Xenopus* embryos is mobilized from $InsP_3$-gated intracellular calcium stores.

Characterization of $InsP_3$-Induced Calcium Release from *Xenopus* Oocyte / Embryo Microsomes

$InsP_3$-induced calcium release from *Xenopus* oocytes and embryos microsomes was characterized. Membrane fraction of *Xenopus* oocytes and embryos were prepared as described in the experimental procedure. Calcium was loaded to microsomes by addition of 2 mM ATP to the microsomes, then various concentration of $InsP_3$ was added and the release of calcium from microsomes was assayed by counting the radioactivity of ^{45}Ca remained in microsomes. Since re-uptake of released calcium was observed to some extent after calcium release, the measurement was carried out enough time (>7 min.) after $InsP_3$ addition in order to obtain the saturated level of calcium release. Dose response curves of $InsP_3$ to release calcium from microsomes of oocytes and embryos were shown in Figure 10. The ability of $InsP_3$ to release calcium was saturated at the concentration of 200nM in microsomes from both the oocytes and embryos. $InsP_3$ was more potent in the microsomes of the embryos than those of the oocytes in the calcium releasing activity: the EC_{50} of $InsP_3$ to release calcium release from oocytes microsomes was 50nM, whereas the EC_{50} of $InsP_3$ to release calcium from

embryo microsomes was 20nM. These results suggest that the calcium stores were sensitized to $InsP_3$ during oocyte maturation or fertilization.

The effect of heparin on calcium release from the *Xenopus* embryos microsomes was studied (Figure 11). $InsP_3$ (100nM)-induced calcium release was inhibited by 100μg/ml of heparin by 70%. De-N-sulfated heparin which was used as control did not affect $InsP_3$-induced calcium release. However, calcium release induced by 1000nM of $InsP_3$ was not inhibited by 100μg/ml of heparin at all (data not shown). Effective dose of heparin against calcium release was rather high compared to its inhibitory activity on $InsP_3$ binding to purified receptors (Parys et al., 1993). Because De-N-sulfated heparin somehow perturbed the cell division cycle *in vivo* at high dose, the modest dose (estimated final concentration: 90μg/ml) of heparin was used in the above experiments .

Expression of $InsP_3$ Receptor during *Xenopus* Embryogenesis

To consider the possibility of the involvement of $InsP_3$ receptors in embryogenesis, expression pattern of the *Xenopus* $InsP_3$ receptor mRNA during *Xenopus* early development was detected by RNase protection assays. $InsP_3$ receptor transcripts are expressed in unfertilized eggs as a maternal products and its amount decreased gradually during the early cleavage stage until late blastula (stage 9)(Figure 12). Its level of expression increased gradually during gastrulation and reached a significant level by the tadpole stage (stage 41).

Expression of $InsP_3$ receptor proteins in embryogenesis was analyzed by western blot analysis using specific polyclonal antisera against *Xenopus* $InsP_3$ receptors. $InsP_3$ receptors were expressed maternally in unfertilized eggs and after fertilization; its level gradually decreased towards gastrulation and then increased again from gastrula stage (Figure 13). The result of western blot analysis shown here correlates well with that of the RNase

protection assays implicating that the $InsP_3$ receptors are regulated at the transcriptional level.

Subcellular Localization of $InsP_3$ Receptors during Cell Cycle

$InsP_3$ receptors are present in the entire region of *Xenopus* oocytes and eggs and are enriched in the perinuclear region in oocytes (Kume et al., 1993). The enrichment in the perinuclear region implicates that the $InsP_3$ receptor may have some role in nuclear division. In order to study its role upon cell division, the localization of $InsP_3$ receptor during cell cycle was examined. Blastomeres at various stages in mitosis at 32 cell-stage embryos are shown in Figure 14. To correlate the stages in cell cycle, DNA was stained with DAPI and the spindle was stained by indirect immunocytochemistry using anti-b-tublin antibody (Amersham N350). The $InsP_3$ receptor-enriched perinucler region surrounded the mitotic apparatus and divided in concert with the motion of separating chromosomes. It may be possible that $InsP_3$ receptor is involved in the regulation of intracellular calcium during mitosis.

Localization of $InsP_3$ Receptors through Development

Localization of $InsP_3$ receptors in early embryos was examined by immunohistochemistry. As shown in Figure 15, $InsP_3$ receptors were localized in the animal hemisphere of 32-cell stage embryo and blastula. In the gastrula stage, expression was observed in the ectoderm including the dorsal lip and the presumptive neuroectoderm. In the early neurula stage (stage 14), expression was observed in the neuroectoderm, notochord, somites, and the epidermis. In stage 24, $InsP_3$ receptors were localized to the neural tube, eye vesicle, lens placote, otic vesicle and notochord. $InsP_3$ receptors were also enriched in the boundaries of the somites. In stage 37/38 tadpoles, they were localized to the floor plate of the neural tube, notochord, somites, pronephros, heart, intestine, and gill. Thus $InsP_3$ receptors were

present in a relatively broad region of embryo which poses the possible role of InsP3 receptor in early development and organogenesis though further studies are needed.

Discussion

Calcium waves and Cleavage

After apparent completion of the first cleavage furrow formation, the calcium waves were consistently observed along the cleavage furrow. But the site of initial rise, the orientation of the wave propagation, the timing and frequency of the rise, and the blastomere in which the calcium wave occurred, varied from egg to egg. Besides these observations, in some cases we observed free calcium rises at the tip of the cleavage furrow, which accompanied the furrow extension. In the absence of extracellular calcium, the calcium waves were consistently observed to follow the first cleavage furrow propagation though the embryo could not survive. The observed patterns of free calcium changes associated with cytokinesis were: (1) rises at progressing cleavage furrow tip, (2) calcium waves following the cleavage furrow progression, and (3) rises at cleavage furrow after the completion of cleavage. Since the amplitude of free calcium changes in embryos which did not survive were larger than that of survived ones, it may be possible that in normal embryos, the patterns (1) and (2) could not be detected constantly in the present system because the amplitude of changes were much smaller.

Fluck et al.(1991) reported two calcium waves at cytokinesis; one followed the cleavage furrow extension and the other with larger amplitude was associated with furrow zipping. It is likely that the calcium waves observed after apparent completion of cleavage is involved in zipping of cleavage furrow. The first cleavage furrow seemed to be zipped after calcium transients (see the images at 28' and 38' in Figures 3 and images of control

embryo at 8' and 28' in Figure 5). On the other hand, the first cleavage furrow in heparin injected embryo did not seem to be zipped (see the heparin-injected embryo at 18' and 38', Figure 5). Sullivan et al.(1993, and unpublished results) has reported the roles of $InsP_3$-induced calcium release in nuclear vesicle fusion of *Xenopus* egg *in vitro*, which suggests its roles in some type of regulated membrane fusion. So, the calcium ion may have roles in zipping the cleavage furrow including the events such as vesicle fusion to increase cell surface, cell adhesion of blastomeres or cytoskeltal changes in cortex.

Formation of Calcium Waves

Calcium waves upon egg fertilization/activation has been reported. Busa and Nuccitelli (1985) detected the Ca^{2+} wave upon activation of *Xenopus* eggs using two calcium-sensitive micro electrodes and estimated the speed of the wave as 9.7 μm/sec at 22°C. Kubota et al.(1987) reported that calcium wave propagated in the cortical cytoplasm of the egg as a wave with a velocity of about 8 μm/sec at 22°C upon prick activation of *Xenopus* eggs. Since the velocity of calcium waves in cytokinesis observed here (2.8 μm/sec at 25-26°C) was much smaller than that in egg activation, there may be different mechanism for the wave propagation in egg activation and in cytokinesis of *Xenopus*..

Free Calcium Oscillation and Cell Cycle Regulation

The present study showed the oscillation of free calcium with the comparable periodicity of cell cycle of *Xenopus* embryos was independent of extracellular calcium and was inhibited by an $InsP_3$ receptor blocker, heparin. Kubota et al.(1993) reported that at the peak of oscillation the embryos were in mitosis. There are few reports which hints the relationship between the calcium transient and cell cycle regulator. As for the downstream targets of calcium

signaling, calmodulin dependent protein kinase II has been shown to mediate inactivation of MPF (M-phase/Maturation promoting factor) (Lorca et al., 1993). Picard et al.(1990) reported that injection of PSTAIR, a peptide of a conserved sequence of $p34^{cdc2}$ into *Xenopus* oocyte induced mobilization of free calcium from intracellular calcium stores although the mechanism is unknown. Although it is tempting to correlate calcium oscillation with cdc2 kinase activity, Ciapa et al.(1993) showed that the calcium oscillation observed during cell cycle progression of sea urchin embryo retained even in the presence of protein synthesis inhibitor, suggesting that the calcium/$InsP_3$ oscillation is independent of mitotic kinase activity. Thus, it is not clear if the oscillation of free calcium is linked to the activity of cell cycle regulators such as cdc2 kinase whose activity could be separated from mitotic events of *Xenopus laevis* (Kimelman et al., 1987, Gerhart et al., 1984, Hara et al., 1980). The mechanism of endogenous activation of PI-turn over and its relationship to cell cycle regulator remains to be elucidated.

Endogenous Activation of $InsP_3$ Receptor-Mediated Calcium Signaling during Cell Cycle Progression

Although the roles of $InsP_3$ as a second messenger to transduce signals across the plasma membrane are established, there are few lines of evidence for the roles of $InsP_3$/calcium signaling triggered endogenously. The present study implies the activation of endogenous $InsP_3$/calcium signaling during cell division cycle. Two distinct spatio-temporal patterns of free calcium changes were observed here: one is the calcium waves at the cleavage furrows and the other is free calcium oscillation with the periodicity of cell division cycle not associated with cytokinesis. Both of them were observed even without extracellular calcium and were inhibited by an $InsP_3$ receptor blocker, heparin. $InsP_3$ receptors were present in the entire region of *Xenopus* eggs and embryos, and were especially enriched in the perinuclear region and the

cortex (this study and Kume et al., 1993). The perinuclear structure immunostained with anti-$InsP_3$ antibody surrounded the mitotic apparatus during mitosis and divided in concert with nuclear division. In sea urchin eggs, calcium transients associated with changes in $InsP_3$ mass during cell division cycle has been reported by Ciapa et al.(1994). Divecha et al.(1991) reported the existence of PI-turn over cycle in the nuclei of Swiss 3T3 cells. Recently $InsP_3$ receptor channel activity were detected by patch-clamp technique in isolated *Xenopus* nuclei (Mak and Foskett, 1994). Nuclear membrane fusion of *Xenopus* eggs was shown to be inhibited by heparin *in vitro* (Sullivan et al.,1993). These lines of evidence indicate that $InsP_3$/calcium signaling is endogenously activated and participate in mitosis and cytokinesis.

$InsP_3$-Induced Calcium Release in *Xenopus* Oocytes and Embryos

Microsomes of *Xenopus* oocytes and embryos showed calcium releasing activity triggered by $InsP_3$ which was inhibited by heparin. The EC_{50} of $InsP_3$ to release calcium was 20 nM in embryo microsomes and 50 nM in oocyte microsomes (Figure 10). This results suggest sensitization of calcium stores to $InsP_3$ may occur during maturation or fertilization. Sensitization of the calcium releasing channels during starfish maturation is reported (China et al., 1990). $InsP_3$ receptor is (Made et al., 1988, Michikawa et al., 1994) and can be phosphorylated (Supattapone et al., 1988, Yamamoto et al., 1989). Phosphorylation of purified mouse cerebellum $InsP_3$ receptor by cyclic AMP-dependent kinase has been demonstrated to increase $InsP_3$ receptor channel activity *in vitro* (Nakade et al., 1994). Since there are no significant changes in the expression of InsP3 receptor during oocyte maturation (Kume , unpublished results) sensitization of $InsP_3$ receptor may take place by chemical modifications such as phosphorylation or glycosylation during oocyte maturation or fertilization.

Embryogenesis and cell signaling

Embryogenesis is thought to be consist of continuously successive cell-cell interactions, or inductive events. Intensive studies on mesoderm and neural induction have begun to reveal the molecular mechanisms of these events. (Kessler and Melton, 1994).

Vegetal endoderm induces marginal zone to form mesoderm and also confers a dorsal-ventral pattern on mesoderm (Boterenbrood and Nieuwkoop, 1973, Dale and Slack, 1987). Many gene products have been shown to be potent mesoderm inducers. Activin, a member of the TGF-β superfamily, can induce animal pole explants to form dorsal mesodermal tissues (Asashima et al., 1990a, 1990b, Smith et al., 1990, Sokol et al., 1990, Thomsen et al., 1990). Experiments with dominant negative form of activin receptor revealed the involvement of activin or activin-related molecules in mesoderm induction in normal development. Fibroblast growth factor (FGF) induces ventro-lateral mesoderm in animal pole explants, including mesenchyme and small amounts of muscle, but fails to induce dorsal mesoderm and the definitive ventral tissue, blood (Slack et al., 1987, Kimelman and Kirschner, 1987, Slack et al., 1988). In whole embryos a dominant inhibitory receptor of FGF causes defects in trunk and posterior development without affecting anterior development (Amaya et al., 1991, Amaya et al., 1993). In animal pole explant assay, bone morphogenetic protein (BMP) 4 , another member of the TGF-β super family, induces ventral mesodrmal tissues, including blood and ventro-lateral molecular markers (Dale et al., 1992, Jones et al., 1992, Graff et al., 1994). Expression of dominant inhibitory BMP2/4 receptor blocks mesoderm induction by BMP4 in animal pole explants and causes a 'dorsalization' of mesoderm in embryos (Suzuki et al., 1994) indicating its ventralizing activity. Vg1, a third member of the TGF-β, was first identified as one of the gene products whose mRNA was localized to vegetal pole in *Xenopus* oocytes

(Rebagliati et al., 1985, Weeks and Melton, 1987, Mowry and Melton, 1992, Dale et al., 1989, Tannahill and Melton, 1989, Melton, 1987)

Spemann's organizer activity is established by mesoderm induction which in turn 'organizes' dorsal axial structures such as somites and neural tube (Spemann, 1938, Hamburger, 1988). Several genes which execute the activity of Spemann's organizer have been cloned and characterized. *goosecoid* (*gsc*) is a homeobox gene whose expression is restricted to the Spemann's organizer region (Blumberg et al., 1991, Cho et al., 1991). Ectopic expression of *gsc* caused second axis formation demonstrating its activity as a Spemann's organizer (Cho et al., 1991). The product of *noggin* gene is a secreted protein which mimics the Spemann's organizer in dorsalizing *Xenopus* mesoderm (Smith et al., 1993).

The possible involvement of PI turnover in mesoderm induction was implied by the teratogenetic effect of lithium. Lithium chloride is known to perturb the PI turnover and shows teratogenetic effect on amphibian development. The site of the action of lithium are reported to be vegetal ventral side of early cleavage stage embryos. In early stage of amphibian development, bath application of lithium chloride can make exaggerate head or dorso-anterior structures and when injected into ventralized embryos by UV irradiation it can respecify the dorso-anterior structures (Kao et al., 1986, Kao and Elinson, 1989, Cooke and Smith, 1988). Inositol or diacylglycerol analog can rescue the effect of lithium on embryonic axis formation (Busa and Gimlich, 1989). In lithium-treated *Xenopus* embryos, the expression of *gsc* and *noggin* is no more restricted to the Spemann's organizer region but they showed the non-polarized expression at marginal zone (Cho et al., 1991, Smith and Harland, 1992). $InsP_3$ mass increases during mesoderm induction and lithium treatment inhibited the increase (Maslanski et al., 1992). Besides the evidence form the experiments with Lithium, some of the signaling molecules described above have been reported to couple with PI turnover cascade.

PLC-γ was shown to be activated by FGF receptor although it was not required for mesoderm induction by FGF in animal pole explants *in vivo* (Peters et al., 678, Muslin et al., 1994). Activin A has been shown to stimulate PI turnover and cause calcium release from intracellular calcium stores in rat hepatocytes and human FSH-secreting pituitary adenoma cells (Mine et al., 1989, Takano et al., 1992). These findings suggests $InsP_3$ signaling could be directly or indirectly involved in mesoderm induction. In the present study, the $InsP_3$ localization was not polarized in dorso-ventral axis, therefore, there may be polarized PI turnover in the development.

Molecular mechanism of neural induction is less known than mesoderm induction although numerous unrelated substances have been reported to act as neural inducers (Saxen et al., 1989). Recently, an endogenous protein, *noggin* was reported to show neural inducer activity. On the other hand, dominant negative experiments on activin type II receptor revealed that inhibition of activin signalling could lead to neuralization (Hemmati-Brivaulou and Melton, 1994), which suggested the neural induction as a default state without signal cue. And also neural induction can be caused by a natural antagonist of the activin receptor, follistatin, *in vivo* (Hemmati-Brivaulou et al., 1994). As for intracellular signalling, the involvement of protein kinase C (PKC) and cAMP-dependent kinase in *Xenopus* neural induction has been reported (Otte et al., 1988, Otte et al., 1989, Otte and Moon, 1992). Very recently an increase of intracellular calcium concentration in *Pleurodeles waltl* embryo explants was observed when triggered by neural inducer such as a lectin, Con A or phorbol 12-myristate 13-acetate (Moreau et al., 1994) which was inhibited by staurosporine or L-type Ca^{2+} channel antagonist. Conversely, it was demonstrated that to increase intracellular calcium concentration by L-type Ca^{2+} channel agonist or caffeine was sufficient to induce the neuralization. So it is possible that there are $InsP_3$ receptor-mediated intracellular calcium mobilization during neural induction in normal

development of *Xenopus laevis*. The enrichment of $InsP_3$ receptors in the ectoderm in gastrula supports this hypothesis although direct evidence remains to be demonstrated.

Experimental Procedures

Microinjection and Treatment of *Xenopus laevis* Embryos

Xenopus laevis females were injected with 750 U of human chorionic gonadotropin (Sigma). On the following day, the eggs were squeezed into modified Barth's saline (88 mM NaCl, 1.0 mM KCl, 2.4 mM $NaHCO_3$, 15.0 mM Hepes-NaOH, pH7.6, 0.3 mM $CaNO_3$, 0.41 mM $CaCl_2$, 0.82 mM $MgSO_4$, 50 U/ml sodium penicillin, and 50 mg/ml streptomycin sulphate) and fertilized *in vitro* . The jelly layer was removed in Steinberg's solution (60 mM NaCl, 0.67 mM KCl, 0.34 mM $Ca(NO_3)_2$, 0.84 mM $MgSO_4$, 10 mM Hepes) containing 2% cystein, pH7.8. The eggs were incubated at 17°C to slow down the cell cycle progression. Ninety minutes after fertilization the embryos were transfered into Steinberg's solution (pH7.4) containing 5% Ficoll 400 and injected with 20 nl of 0.5 mM Calcium Green-1(Molecular Probe) in injection buffer (88 mM NaCl, 1 mM KCl, 15 mM Tris-HCl, pH7.5). *Xenopus* oocytes were defolliculated manually prior to the dye injections. Eggs were injected in four direction with 5 nl x 4 of the injection solution to assure the uniform diffusion of injected material until measurement. Heparin (MW.3500, Sigma), De-N-sulfated heparin (Sigma) or colchicine (Sigma) was co-injected with the dye when used. When the first cleavage furrow appeared at animal pole, the eggs were washed with the same medium used in the measurement and the dye fluorescent was monitored by confocal microscope.

Confocal Microscopy

Images were acquired on a confocal laser microscope system, Bio-Rad MRC-500 adapted to Olympus inverted microscope, IMT-2 (objective lenses; Plan 4/0.13NA(4x) and Plan 2/0.05NA(2x), Nikon) using CoMOS and TCSM software packages (Bio-Rad Microscience). Ten images were averaged on line by kalman algorithm to produce each image except for images in Figure 4. The images were further processed on Macintosh computers using the public domain NIH Image program (written by Wayne Rasband at the U.S. National Institutes of Health and available from the Internet by anonymous ftp from zippy.nimh.nih.gov or on floppy disk from NTIS, 5285 Port Royal Rd.,Springfield, VA 22161, part number PB93-504868) and IPlab package (Signal Analytics, Vienna, VA) softwares with custom software modules for those programs developed by Dr. Takafumi Inoue. All measurements were carried out at room temperature.

Preparation of Microsomes

Microsomes of *Xenopus* embryos were prepared as described by Parys et al.,1992 with some modifications. *Xenopus* embryos at early cleavage stage (1 to 8 cell-stages) were dejellied, homogenized in 4 volume of ice-cold buffer containing 50 mM of Tris-HCl, pH7.25, 250 mM sucrose, 1 mM EGTA, 1 mM DTT, 0.1 mM PMSF, 10 mM leupeptin, and 1 mM pepstatin A, by 4 strokes in a 20-ml glass-Teflon homogenizer. The homogenate was centrifuged at 4500xg (Tomy No.4 rotor, 6,000r.p.m.) for 15 min. The supernatant was centrifuged at 55,000 r.p.m. for 35 min. in TLA100.3 rotor (BECKMAN) at 2°C. The pellet was resuspended in ice-cold buffer containing 20 mM Tris-HCl, pH7.25, 300 mM sucrose, 1 mM EGTA, 1mM DTT, 0.1m M PMSF, 10 mM leupeptin, and 1 mM pepstatin A, and was frozen in liquid nitrogen and stored at -80°C until use.

Calcium Release from Microsomes

The microsomes were thawed, pelleted at 100,000 r.p.m. for 15 min. at 2°C in TLA100.2 rotor (BECKMAN), resuspended by pipetting in buffer containing 10 mM Hepes, pH7.2, 110 mM KCl, 10 mM NaCl, 1mM $MgCl_2$, 5 mM KH_2PO_4, 1mM DTT, 0.1mM PMSF, 10 mM leupeptin and 1mM pepstatin A and 200mM free calcium which were buffered in Ca-EGTA buffer (Methods in Enzymology 172, pp230-262). The microsome fraction was adjusted to a final concentration of 1mg protein/ml. ^{45}Ca(NEN/DU PONT) was then added at the concentration of 8 or 24 mCi/ml. Calcium uptake was initiated by adding 2 mM ATP and allowed to be saturated for more than 20 min at 20°. Heparin, an $InsP_3$ receptor antagonist, was added 20 min. after ATP addition. Then $InsP_3$ was added and 20 ml of aliquot was taken, spotted onto 0.45-μm filter (Type HA, NIHON MILLIPORE). The filter were dried thoroughly, soaked into 6ml of AQUASOL-2 (NEN/DU PONT) and assayed by scintillation counting.

RNase Protection Analysis

RNA was extracted from embryos at each stage by vanadyl-complex method (Berger and Birkenmeier, 1979). Total RNA was hybridized with an RNA probe for *Xenopus* $InsP_3$ receptor and analyzed by RNase protection studies basically according to the method described previously (Melton et al., 1984, Okano et al., 1988). cDNA *Pvu* II 0.66 kb fragment (5233-5906bp, Kume et al., 1993) was subcloned into *Eco* RI site of pBluscript KS(-) vector (Stratagene) to give XpB14*Pvu* II and the labeled anti-sense RNA probes was synthesized by adding T7 RNA polymerase (Boehringer Mannheim) to XpB14*Pvu* II linearized with *Sal* I, in the presence of ^{32}P-UTP (800 Ci/mmol, Amersham). Aliquots of 2x10^6 c.p.m. of the probe was hybridized to 20 μg of total RNA (at 42°C for 12 hours) and yeast tRNA controls in a solution containing 80% formamide, 40 mM PIPES, 0.4 M NaCl, and 1mM EDTA. The unhybridized regions of the probe was digested with 100 ng of RNase A and

20U of RNase T1 at 17°C for 30 minutes in a total volume of 0.35 ml, followed by phenol chloroform extraction and ethanol precipitation. The length of the RNase-resistant ^{32}P-RNA-RNA hybrids was analyzed by electrophoresis on denaturing 5% polyacrylamide-8M urea gel. In addition, unprotected RNA probe was applied to the gel electrophoresis as a reference.

Western Blot Analysis

Crude membrane proteins from *Xenopus* embryos were prepared as follows: *Xenopus* embryos were mixed with about 9 volume of the solution containing 0.32 M sucrose, 1mM EDTA, 0.1mM PMSF, 10mM leupeptin, 10mM pepstain A, 1mM β-ME and 50 mM Tris-HCl (pH8.0). The mixture was homogenized in 1.5 ml eppendorf tube. The homogenate was centrifuged at 1000g for 15 min. at 2°C. The supernatants were centrifuged at 105,000g for 15 minutes at 2°C. The precipitates was electrophoresed on 5%-SDS polyacrylamide gel according to the method of Laemmli (1970) and transferred to a nitrocellulose filter. The blots were immunostained with antiserum against GST-*Xenopus* $InsP_3$ receptor (1/100 dilution) by using Vectastain ABC rabbit IgG kit according to the manufacturer's protocol, and finally visualized with 1mg/ml 3,3'-diaminobenzidine, tetrahydrochloride, 0.02% H_2O_2.

Preparation of GST-*Xenpus* $InsP_3$ Receptor Fusion Protein

Antigen used for immunization was prepared as follows. A cDNA fragment (7764-8271b.p., Kume et al., 1993) encoding 155 amino acid residue of the C-terminal (2539-2693 amino acid residue) which corresponds to C-terminal cytoplasmic domain was amplified by the polymerase chain reaction using a pair of primers constructed on the basis of the sequence of *Xenopus* InsP3 receptor according to the standard method (Saiki et al., 1988). The sequences of primers used are 5'-GGA ATT CTG AGG AGT GAG AAG CAA AAG-3' and 5'-CGA ATT CTA AAA TGG GCA GCA GGT GTG G-3'. The

amplified fragment was subcloned into pGEX-2T vector (Smith and Johnson, 1986) at *Eco* RI site to obtain pGEX-*Xenopus* InsP3 to generate GST fusion protein. The amplified cDNA was sequenced. *Escherichia coli* JM109 transformed with pGEX-InsP$_3$ receptor DNA construct were grown at 37°C to the logarithmic phase and treated with 1mM IPTG for 4--6hr. Then the bacteria were harvested and the crude extracts were electrophoresed in 10% SDS-polyacrylamide gel. The gel were rinsed with ice-cold distilled water, soaked in 0.25M KCl containing 2 mM b-ME for staining of the gel. The band corresponding to GST-*Xenopus* InsP3 receptor was excised and the proteins were collected by electroelution.

Raising antisera against *Xenopus* InsP3 Receptor

Rabbits were treated subcutaneously with 170μg of the purified GST-*Xenopus* InsP$_3$ receptor fusion protein in Freund's complete adjuvant (1:1) at 2 week intervals. After the fourth booster injection, sera were collected and checked for immunoreactivity to *Xenopus* InsP$_3$ receptor. A major band corresponding to the *Xenopus* InsP$_3$ receptor was detected by immunoblot analysis of the crude membrane proteins of the *Xenopus* oocytes using the antiserum.

Cytology and Immunocytochemistry

The embryos were fixed in ice-cold 4% paraformaldehyde in PBS (137 mM NaCl, 2.5 mM KCl, 8 mM Na_2HPO_4, 1.5 mM KH_2PO_4) for 2 hr, dehydrated, parrafin-embedded and sectioned with the thickness of 6 μm. For DNA staining, the sections were stained with 1μg/ml DAPI for 10 min. Antiserum against GST-*Xenopus* InsP$_3$ receptor fusion protein (Kume et al., 1993) were diluted to 1/100 and used for detection of IP$_3$ receptors. Fluorescein-conjugated or rhodamin-conjugated anti-rabbit IgG(H+L) antibody (Vector) were used for secondary antibodies. Anti-β-tublin antibody (Amersham) was used to stain spindles. Fluorescein-conjugated anti-mouse IgG(H+L) antibody (Vector) was used for secondary antibody.

Acknowledgments

I would like to thank Prof. Mikoshiba, Prof. Asano and Prof. Okano for encouragement, to Dr. Kume for reading the manuscript and discussion, and to Dr. Inoue for technical support and discussion. I also wish to express my gratitude to everyone in Mikoshiba's laboratory for encouragement.

References:

Amaya, E., Musci, T.J., and Kirschner, M.W. (1991). Expression of a dominant negative mutant of the FGF receptor disrupts mesoderm formation in *Xenopus* embryos. Cell 66, 257-270.

Amaya, E., Stein, P.A., Musci, T.J., and Kirschner, M.W. (1993). FGF signaling in the early specification of mesoderm in *Xenopus*. Development 118, 477-487.

Arnold, J.M. (1975). An effect of calcium in cytokinesis as demonstrated with ionophore A23187. Cytobiologie 11, 1-9.

Asashima, M. (1990). The vegetalizing factor belongs to a family of mesoderm-inducing proteins related to erythroid differentiation factor. Naturwissenschaften 77, 389-391.

Asashima, M., Nakano H, K, S., K, K., K, I., H, S., and N, U. (1990). Mesodermal induction in early amphibian embryos by activin A(erythroid differentiation factor). Roux's Arch. Dev. Biol. 198, 330-335.

Berger, S.L., and Birkenmeier, C.S. (1979). Inhibition of intractable nucleases with ribonucleoside-vanadyl complexes: Isolation of messenger ribonucleic acid from resting lymphocytes. Biochemistry 18, 5143.

Berridge. (1993). Inositol trisphosphate and calcium signalling. Nature 361, 315-325.

Berridge, M.J., Downes, C.P., and Hanley, M.R. (1989). Neural and Developmental Actions of Lithium: A Unifying Hypothesis. Cell 59, 411-419.

Blumberg, B., Wright, C.V.E., DeRobertis, E.M., and Cho, K.W.Y. (1991). Organizer-specific homeobox genes in Xenopus laevis embryos. Science 253, 194-196.

Boterenbrood, E.C., and Nieuwkoop, P.D. (1973). The formation of the mesoderm in urodelean amphibians. V. Its regional induction by the endoderm. Roux's Arch. Entwicklungsmech. Org. 173, 319-332.

Busa, W.B. (1988). Roles for the phosphatidylinositol cycle in early development. Phil. Trans. R. Soc. Lond. B 320, 415-426.

Busa, W.B., and Gimlich, R.L. (1989). Lithium-Induced Teratogenesis in Frog Embryos Prevented by a Polyphosphoinositide Cycle Intermediate or a Diacylglycerol Analog. Dev. Biol. 132, 315-324.

Busa, W.B., and Nuccitelli, R. (1985). An elevated free cytosolic Ca^{2+} wave follows fertilization in eggs of the frog, Xenopus laevis. J. Cell Biol. 100, 1325-1329.

Chiba, K., Kado, R.T., and Jaffe, L.A. (1990). Development of calcium release mechanisms during starfish oocyte maturation. developmental biology 140, 300-306.

Cho, K.W.Y., Blumberg, B., Steinbeisser, H., and DeRobertis, E.M. (1991). Molecular nature of Spemann's organizer: the role of the Xenopus homeobox gene *goosecoid.* Cell 67, 1111-1120.

Ciapa, B., Pesando, D., Wilding, M., and Whitaker, M. (1994). Cell-cycle calcium transients driven by cyclic changes in inositol trisphosphate levels. Nature 368, 875-878.

Conrad, G.W., Glackin, P.V., Hay, R.A., and Patron, R.P. (1987). Effects of calcium antagonists, calmodulin antagonists, and methylated xanthines on polar lobe formation and cytokinesis in fertilized eggs of Ilyanassa obsoleta. J. Exp. Zool. 243, 245-258.

Cooke, J., and Smith, E.J. (1988). The restrictive effect of early explosure to lithium upon body pattern in Xenopus development, studied by quantitative anatomy and immunofluorescence. Development 102, 85-99.

Dale, L., Howes, G., Price, B.M.J., and Smith, J.C. (1992). Bone morphogenetic protein 4: a ventralizing factor in early *Xenopus* development. Development 115, 573-585.

Dale, L., Matthews, G., Tabe, L., and Colman, A. (1989). Developmental expression of the protein product of Vg1, a localized maternal mRNA in the frog Xenopus laevis. EMBO J. 8, 1057-1065.

Dale, L., and Slack, J.M.W. (1987). Regional specification within the mesoderm of early embryos of *Xenopus laevis*. Development 100, 279-295.

Davis, M. (1988). Protein kinases in amphibian ectoderm induced for neural differentiation. Roux's Arch. Dev. Biol. 197, 339-344.

DeLisle, S., and Welsh, M.J. (1992). Inositol Trisphosphate Is Required for the Propagation of Calcium Waves in Xenopus Oocytes. J. Biol. Chem. 267, 7963-7966.

Divecha, N., Banfic, H., and Irvine, R.F. (1991). The polyphosphoinositide cycle exists in the nuclei of Swiss 3T3 cells under the control of a receptor (for IGF-1) in the plasma membrane, and stimulation of the cycle increases nuclear diacylglycerol and apparently induces translocation of protein kinase C to the nucleus. EMBO J. 10, 3207-3214.

Fluck, R.A., Miller, A.L., and Jaffe, L.F. (1991). Slow Calcium Waves Accompany Cytokinesis in Medaka Fish Eggs. J. Cell Biol. 115, 1259-1265.

Galione, A., McDougall, A., Busa, W.B., Willmott, N., Gillot, I., and Whitaker, M. (1993). Redundant mechanisms of calcium-induced calcium release underlying calcium waves during fertilization of sea urchin eggs. Science 261, 348-352.

Gerhart, J., Wu, M., and Kirschner, M. (1984). Cell cycle dynamics of an M-phase-specific cytoplasmic factor in Xenopus laevis oocytes and eggs. J. Cell Biol. 98, 1247-1255.

Grandin, N., and Charbonneau, M. (1991). Intracellular Free Calcium Oscillates during Cell Division of Xenopus Embryos. J. Cell Biol. 112, 711-718.

Hamburger, V. (1988). The heritage of experimental embryology. Oxford University Press. Oxford, England.

Han, J.-K., Fukami, K., and Nuccitelli, R. (1992). Reducing Inositol Lipid Hydrolysis, Ins(1,4,5)P3 Receptor Availability, or Ca2+ Gradients Lengthens the Duration of the Cell Cycle in Xenopus laevis Blastomeres. J. Cell Biol. 116, 147-156.

Hara, K., Tydeman, P., and Kirschner, M. (1980). A cytoplasmic clock with the same period as the division cycle in Xenopus eggs. Proc. Natl. Acad. Sci. USA 77, 462-466.

Hemmati-Brivanlou, A., Kelly, O.G., and Melton, D.A. (1994). Follistatin, and antagonist of activin, is expressed in the Spemann organizer and displays direct neuralizing activity. Cell 77, 283-295.

Hemmati-Brivanlou, A., and Melton, D.A. (1994). Inhibition of activin receptor signaling promotes neuralization in Xenopus. Cell 77, 273-281.

Hepler, P.K. (1994). The role of calcium in cell division. Cell Calcium 16, 322-330.

Jones, C.M., Lyons, K.M., Lapan, P.M., Wright, C.V.E., and Hogan, B.J.M. (1992). DVR-4(bone morphogenetic protein-4) as a posterior ventralizing factor in *Xenopus* mesoderm induction. Development 115, 639-647.

Kao, K.R., and Elinson, R.P. (1989). Dorsalization of mesoderm induction by lithium. Dev. Biol. 132, 81-90.

Kao, K.R., Masui, Y., and Elinson, R.P. (1986). Lithium-induced respecification of pattern in Xenopus laevis embryos. Nature 322, 371-373.

Kessler, D.S., and Melton, D.A. (1994). Vertebrate embryonic induction: mesodermal and neural patterning. Nature 266, 596-604.

Kimelman, D., and Kirschner, M. (1987). Synergistic induction of mesoderm by FGF and TGFβ and the identification of an mRNA coding for FGF in the early *Xenopus* embryo. Cell 51, 369-377.

Kimelman, D., Kirschner, M., and Scherson, T. (1987). The events of the midblastula transition in Xenopus are regulated by changes in the cell cycle. Cell 48, 399-407.

Kubota, H.Y., Yoshimoto, Y., Yoneda, M., and Hiramoto, Y. (1987). Free Calcium Wave upon Activation in Xenopus Eggs. Dev. Biol. 119, 129-136.

Kume, S., Muto, A., Aruga, J., Nakagawa, T., Michikawa, T., Furuichi, T., Nakade, S., Okano, H., and Mikoshiba, K. (1993). The Xenopus IP3 Receptor: Structure, Function, and Localization in Oocytes and Eggs. Cell 73, 555-570.

Laemmli, U.K. (1970). Cleavage of structural proteins during the assembly of the head of bacteriophage T4. Nature 227, 680-685.

Larabell, C., and Nuccitelli, R. (1992). Inositol Lipid Hydrolysis Contributes to the Ca^{2+} Wave in the Activating Egg of Xenopus laevis. Dev. Biol. 153, 347-355.

Lee, H.C., Aarhus, R., and Walseth, T.F. (1993). Calcium mobilization by dual receptors during fertilization of sea urchin eggs. Science 261, 352-355.

Lorca, T., Cruzalegui, F.H., Fesquet, D., Cavadore, J.-C., Mery, J., Means, A., and Doree, M. (1993). Calmodulin-dependent protein kinase II

mediates inactivation of MPF and CSF upon Fertilization of Xenopus eggs. Nature 366, 270-273.

Maeda, N., Niinobe, M., Nakahira, K., and Mikoshiba, K. (1988). Purification and characterization of P400 protein, a glyco-protein characteristic of Purkinje cell, from mouse cerebellum. J. Neurochem. 51, 1724-1730.

Mak, D.-O.D., and Foskett, J.K. (1994). Single-channel Inositol 1,4,5-Trisphosphate Receptor Currents revealed by Patch Clamp of Isolated Xenopus Oocyte Nuclei. J. Biol. Chem. 269, 29375-29378.

Maslanski, J.A., Leshko, L.A., and Busa, W.B. (1992). Lithium-sensitive production of inositol phosphates during amphibian embryonic mesoderm induction. Science 256, 243-245.

Melton, D.A. (1987). Translocation of a localized maternal mRNA to the vegetal pole of *Xenopus* oocytes. Nature 328, 80-82.

Melton, D.A., Krieg, P.A., Rebagliati, M.R., Maniatis, T., Xinn, K., and Green, M.R. (1984). Efficient in vitro synthesis of biologically active RNA and RNA hybridization probes from plasmids containing a bacteriophage SP6 promoter. Nucleic. Acids Res. 12, 7035-7056.

Michikawa, T., Hamanaka, H., Otsu, H., Yamamoto, A., Miyawaki, A., Furuichi, T., Tashiro, Y., and Mikoshiba, K. (1994). Transmembrane Topology and Sites of N-Glycosylation of Inositol 1,4,5-Trisphosphate Receptor. J. Biol. Chem. 269, 9184-9189.

Mine, T., Kojima, I., and Ogata, E. (1989). Stimulation of glucose production by Activin-A in isolated rat hepatocytes. Endocrinology 125, 586-.

Mine, T., Kojima, I., and Ogata, E. (1992). Pertussis toxin blocks Activin A- induced production of inositol phosphates in rat hepatocytes. Biochemical and Biophysical Research Communications 186, 205-210.

Minshull, J., Sun, H., Tonks, N.K., and Murray, A.W. (1994). A MAP Kinase-Dependent Spindle Assembly Checkpoint in Xenopus Egg Extracts. Cell 79, 475-486.

Miyazaki, S.-i., Yuzaki, M., Nakada, K., Shirakawa, H., Nakanishi, S., Nakade, S., and Mikoshiba, K. (1992). Block of Ca2+ wave and Ca2+ oscillation by antibody to the inositol 1,4,5-trisphosphate receptor in fertilized hamster eggs. Science 257, 251-255.

Mohammadi, M., Dionne, C.A., Li, W., Spivak, T., Honegger, A.M., Jate, M., and Schlessinger, J. (1992). Point mutation in FGF receptor eliminates phosphatidylinositol hydrolysis without affecting mitogenesis. Nature 358, 681-684.

Mowry, K.L., and Melton, D.A. (1992). Vegetal messenger RNA localization directed by a 340-nt RNA sequence element in Xenopus oocytes. Science 255, 991-994.

Muto, A. (1992). Primary structure and immunolocalization of InsP3 receptor in oocytes/eggs of *Xenopus laevis*. Masteral Thesis, Osaka University

Nakade, S., Rhee, S.K., Hamanaka, H., and Mikoshiba, K. (1994). Cyclic AMP-dependent Phosphorylation of an Immunoaffinity-purified Homotetrameric Inositol 1,4,5-Trisphosphate Receptor (Type I) Increases Ca^{2+} Flux in Reconstituted Lipid Vesicles. J. Biol. Chem. 269, 6735-6742.

Nieuwkoop, P.D. (1969). The formation of mesoderm in Urodelean amphibia. I. Induction by the endoderm. Wilhem Roux Arch. EntwMech. Org. 162, 341-373.

Nieuwkoop, P.D., and Faber, J. (1967). The normal development table of Xenopus laevis. North-Holland Publishing Company. Amsterdam.

Nuccitelli, R., Yim, D.L., and Smart, T. (1993). The Sperm-induced Ca2+ wave following fertilization of the Xenopus egg requires the production of Ins(1,4,5)P3. Developmental Biology 158, 200-212.

Okano, H., Ikenaka, K., and Mikoshiba, K. (1988). Recombination within the upstream gene of duplicated myelin basic protein genes of myelin deficient shi-mld mouse results in the production of antisense RNA. EMBO J. 7, 3407-3412.

Otte, A.P., Koster, C.M., Snoek, G.T., and Durston, A.J. (1988). Protein kinase C mediates neural induction in Xenopus laevis. Nature 324, 618-620.

Otte, A.P., and Moon, R.T. (1992). Protein kinase C isozymes have distinct roles in neural induction and competence in Xenopus. Cell 68, 1021-1029.

Otte, A.P., Van Run, P., Heldelveld, M., Rian-Driel, R., and Durston, A.J. (1989). Neural induction is mediated by cross-talk between the protein kinase C and cyclic AMP pathways. Cell 58, 641-648.

Paine, P.L. (1984). Diffusive and nondiffusive proteins in vivo. J. Cell Biol. 99, 188-195.

Parys, J.B., Sernett, S.W., DeLisle, S., Snyder, P.M., Welsh, M.J., and Campbell, K.P. (1992). Isolation, Characterization, and Localization of the Inositol 1,4,5-Trisphosphate Receptor Protein in Xenopus laevis Oocytes. J. Biol. Chem. 267, 18776-18782.

Picard, A., Cavadore, J.-C., Lory, P., Bernengo, J.-C., Ojeda, C., and Doree, M. (1990). Microinjection of a conserved peptide sequence of $p34^{cdc2}$ induces a Ca2+ transient in oocytes. Science 247, 327-329.

Poenie, M., Alderton, J., Tsien, R.Y., and Steinhardt, R.A. (1985). Changes of free calcium levels with stages of the cell division cycle. Nature 315, 147-149.

Rebagliati, M.R., Weeks, D.L., Harvey, R.P., and Melton, D.A. (1985). Identification and cloning of localized maternal RNAs from Xenopus eggs. Cell 42, 769-777.

Saiki, R.K., Gelfand, D.H., Stoffel, S., Scharf, S.J., Higuchi, R., Horn, G.T., Mulls, K.B., and Erlich, H.A. (1988). Primer-directed enzymatic amplification of DNA with a thermostable DNA polymerase. Science 239, 487-491.

Saxen, L. (1989). Neural induction. Int. J. Dev. Biol. 33, 21-48.

Slack, J.M.W., Darlington, B.G., Heath, J.K., and Godsave, S.F. (1987). Mesoderm induction in early *Xenopus* embryos by heparin-binding growth factors. Nature 326, 197-200.

Slack, J.M.W., Isaacs, H.V., and Darlington, B.G. (1988). Inductive effects of fibroblast growth factor and lithium ion on *Xenopus* blastula ectoderm. Development 103, 581-590.

Smith, J.C., Price, B.M.J., Nimmen, K.V., and Huylebroeck, D. (1990). Identification of a potent *Xenopus* mesoderm-inducing factor as a homolog of activin A. Nature 345, 729-731.

Smith, R.B., and Johnson, K.S. (1986). Single-step purificaion of polypeptides expressed in Escherichia coli as fusions with glutathione S-transferase. Gene 67, 31-40.

Smith, W.C., and Harland, R.M. (1992). Expression cloning of noggin, a new dorsalizing factor localized to the Spemann organizer in Xenopus embryos. Cell 70, 829-840.

Smith, W.C., Knecht, A.K., Wu, M., and Harland, R.M. (1993). Secreted noggin protein mimics the Spemann organizer in dorsalizing Xenopus mesoderm. Nature 361, 547.

Snow, P., and Nuccitelli, R. (1993). Calcium Buffer Injections Delay Cleavage in Xenopus laevis Blastomeres. J. Cell Biol. 122, 387-394.

Sokol, S., Wong, G.G., and Melton, D.A. (1990). A mouse macrophage factor induces head structures and organizes a body axis in *Xenopus*. Science 249, 561-564.

Spemann, H. (1938). Embryonic development and induction. Yale University Press. New Haven, Connecticut.

Stith, B.J., Goalstone, M., Silva, S., and Jaynes, C. (1993). Inositol 1,4,5-Trisphosphate Mass Changes from Fertilization Through First Cleavage in Xenopus laevis. Molecular Biology of the Cell 4, 425-443.

Sullivan, K.M.C., Busa, W.B., and Wilson, K.L. (1993). Calcium Mobilizaiton Is Required for Nuclear Vesicle Fusion In Vitro: Implications for Membrane Traffic and IP3 Receptor Function.

Supattapone, S., Danoff, S.K., Theibert, A., Josefh, S.K., Steiner, J., and Snyder, S.H. (1988). Cyclic AMP-dependent phosphorylation of a brain inositol trisphosphate receptor decreases its release of calcium. Proc. Natl. Acad. Sci. USA 85, 8747-8750.

Suzuki, A., Thies, R.S., Yamaji, N., Song, J.J., Wozney, J.M., Murakami, K., and Ueno, N. (1994). A truncated bone morphogenetic protein receptor affects dorsal-ventral patterning in the early Xenopus embryo. Proc. Natl. Acad. Sci. USA 91, 10255-10259.

Takano, K., Yamashita, N., Kojima, I., Kitaoka, M., Teramoto, A., and Ogata, E. (1992). Effects of activin A and somatostatin of intact FSH secretion and intracellular Ca^{2+} concentration in human FSH-secreting pituitary adenoma cells. Biochem. Biophys. Res. Comm. 182, 1408-1415.

Tannahill, D., and Melton, D.A. (1989). Localized synthesis of the Vg1 protein during early Xenopus development. Development 106, 775-785.

Thomsen, G., Woolf, T., Whitman, M., Sokol, S., Vaughan, J., Vale, W., and Melton, D.A. (1990). Activins are expressed early in Xenopus

embryogenesis and can induce axial mesoderm and anterior structures. Cell 63, 485-493.

Weeks, D.L., and Melton, D.A. (1987). A maternal mRNA localized to the vegetal hemisphere in Xenopus eggs codes for a growth factor related to TGF-beta. Cell 51, 861-867.

Yamamoto, H., Maeda, N., Niinobe, M., Miyamoto, E., and Mikoshiba, K. (1989). Phosphorylation of P400 protein by cyclic AMP-dependent protein kinase and Ca^{2+}/calmodulin-dependent protein kinase II. J. Neurochem. 53, 917-923.

Figure 1. Calcium Green-1 Fluorescence

The intensity of Calcium Green-1 fluorescence at various concentration of free calcium with or without 200 μg/ml of heparin or De-N-sulfated heparin was measured. The value of the fluorescence at zero calcium was subtracted from each value. The intensity was measured by Bio-Rad confocal microscope which was used for calcium-imaging of *Xenopus* embryos. The fluorescence was not affected by either heparin or De-N-sulfated heparin.

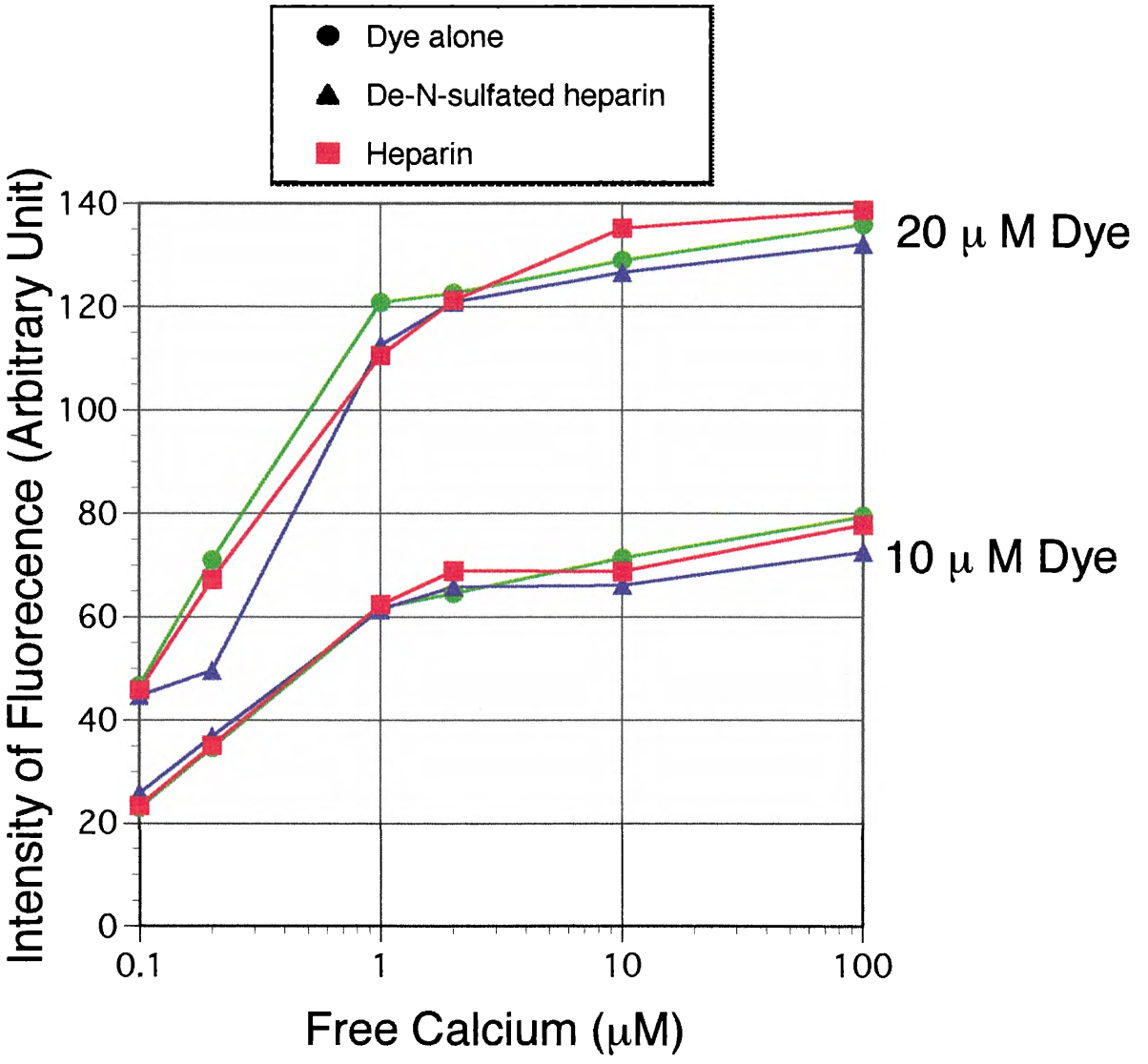
Dye alone
De-N-sulfated heparin
Heparin
Intensity of Fluorecence (Arbitrary Unit)
140
120
100
80
60
40
20
0
0.1
1
10
100
Free Calcium (μM)
20 μ M Dye
10 μ M Dye

Figure 2. Fluorescence of Oocyte after Dye Injection

Oocytes were injected with 20nl of 0.5mM Calcium Green-1 at the equatorial region near the animal pole in four directions. Eight minutes after injection, the fluorescence was monitored from the vegetal side with an Nikon 2x /0.05NA objective lens at 24°C The extracellular medium was Modified Barth's saline. Focal plane was adjusted to 200 μm toward the vegetal pole from the equator of the oocyte. The confocal aperture was set to the fully open state to maximize the detectable fluorescence. The averaged intensity of the fluorescence over the entire region of the oocyte was plotted as F/F(60min) , since in the following studies, the measurement was started about 60 minutes after dye injection. Note that the intensity does not reach its plateau even 3 hours after dye injection

.

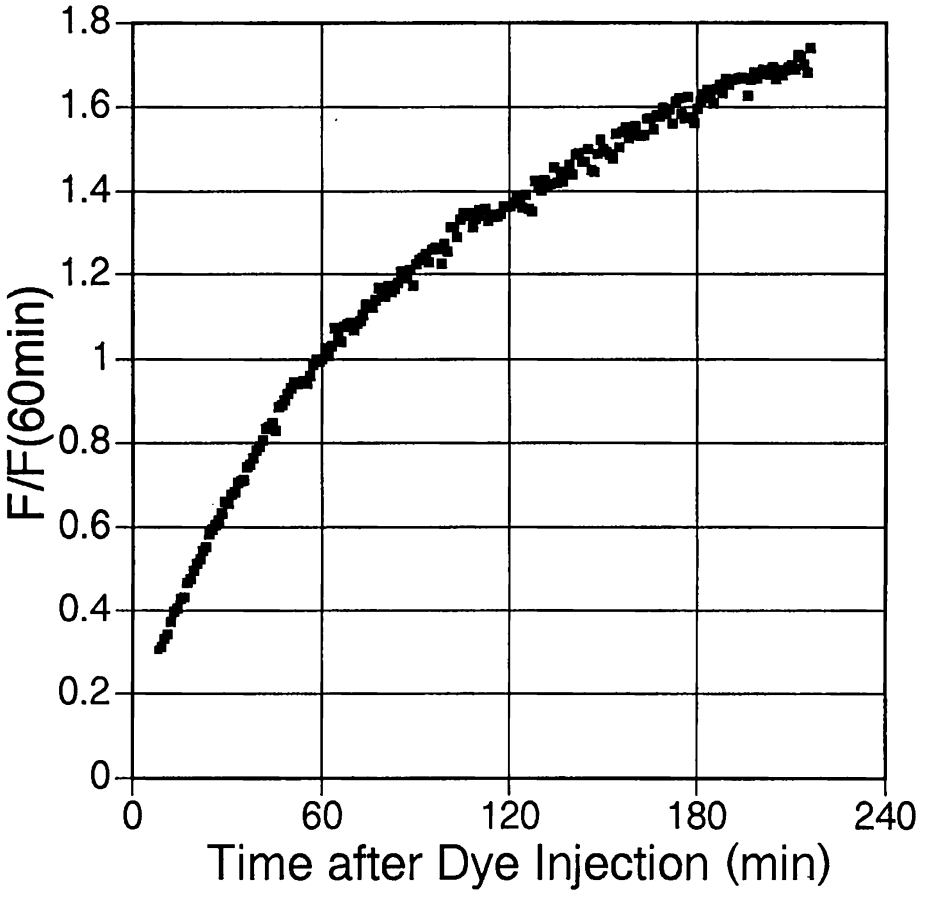
1.8
1.6
1.4
1.2
1
0.8
0.6
0.4
0.2
0
F/F(60min)
0
60
120
180
240
Time after Dye Injection (min)

Figure 3. Calcium Waves Occurs at Cleavage Furrow

After fertilization the calcium indicator dye, Calcium Green-1 was injected and after the onset of the first cleavage the embryos was observed with confocal microscopy using Nikon 4x/0.13NA objective lens. The focal plane was determined to maximize the detectable fluorescence. The confocal aperture was set to the fully open condition. The measurement was started when the first cleavage furrow was progressing at the equatorial region. The time at which the measurement was started is taken as time 0' in the following experiments. Room temperature, 25 °C.

(a)The fluorescent images of *Xenopus* embryo at 1 cell- to 4 cell-stage are shown. This measurement was carried out in 1/50 Steinberg's solution. The embryo shown here developed to tadpole stage.

(b)The averaged fluorescence in the indicated regions of the same embryo. Averaged fluorescence plotted as F/F0 where F0 is the fluorescence at time 0'. The region in green is just beside the first cleavage furrow and the region in red is beside the second cleavage furrow. Note that the sharp peak at 32' in green corresponds to the rise at the first cleavage furrow. At the time point of 20', F/F0 in both regions reached a peak which is not associated with any rises at cleavage furrow. This corresponds to the first peak of free calcium oscillation shown in Figure 8 (see below).

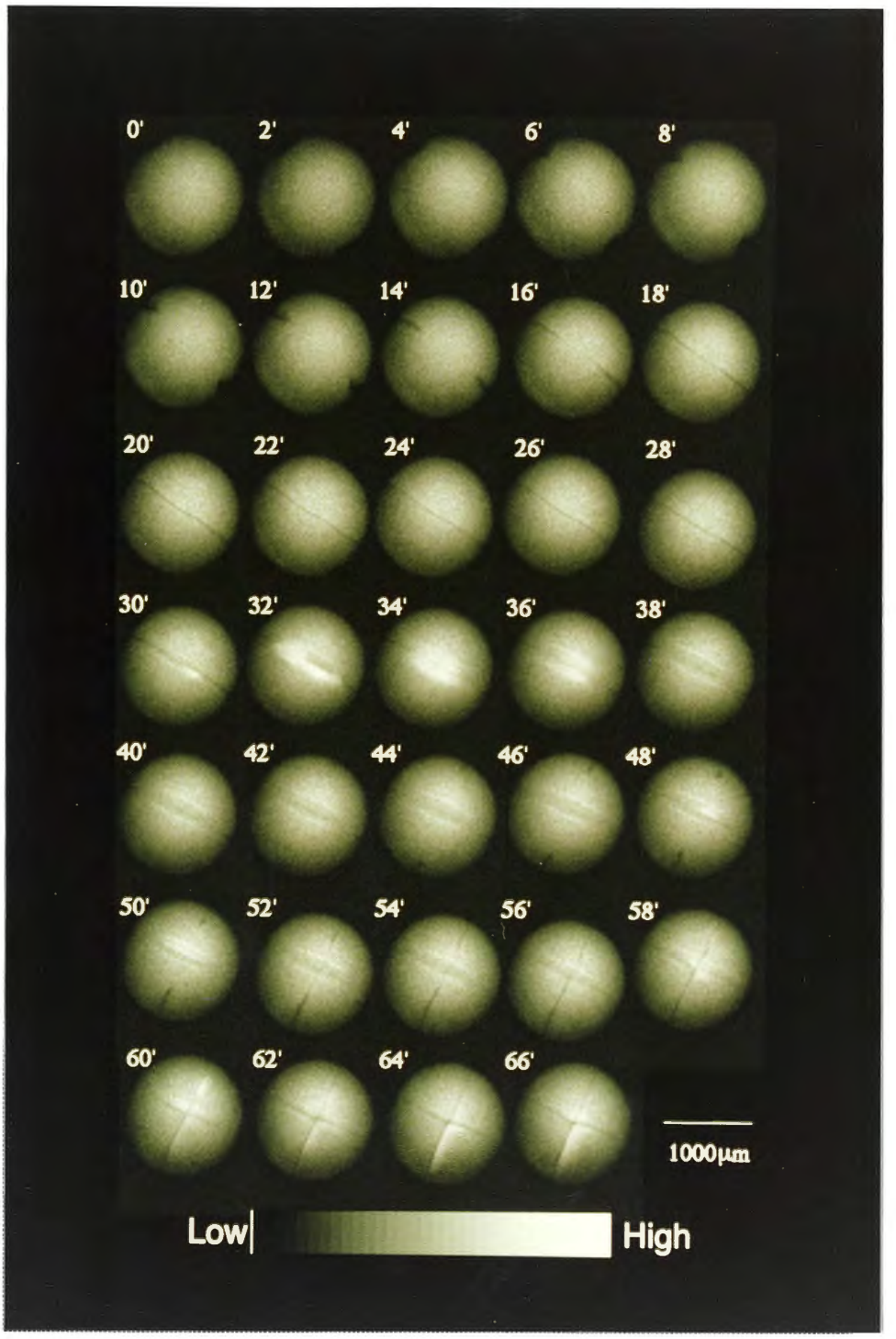
0'
2'
4'
6'
8'
10'
12'
14'
16'
18'
20'
22'
24'
26'
28'
30'
32'
34'
36'
38'
40'
42'
44'
46'
48'
50'
52'
54'
56'
58'
60'
62'
64'
66'
1000μm
Low
High

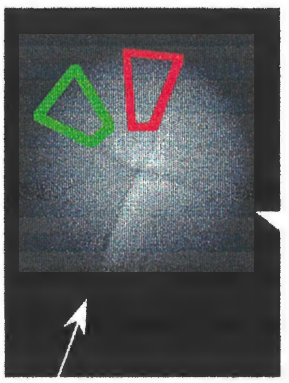
1st cleavage furrow
2nd cleavage furrow

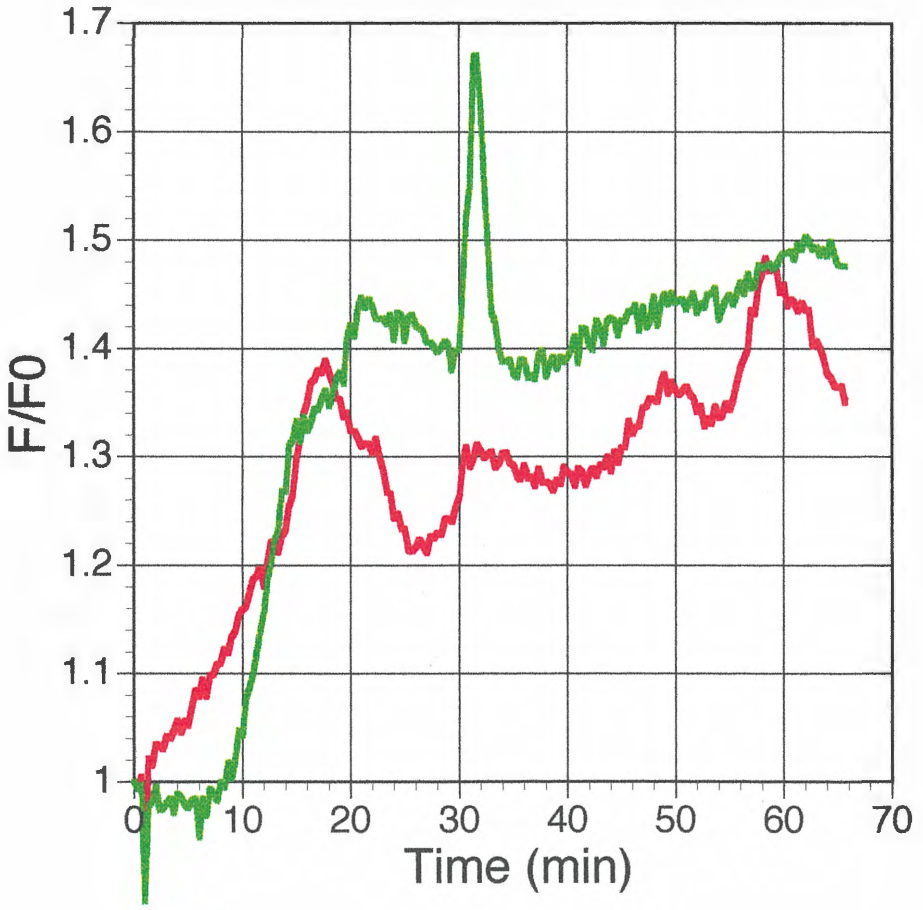
F/F0
1.7
1.6
1.5
1.4
1.3
1.2
1.1
1
0
10
20
30
40
50
60
70
Time (min)

Figure 4. Calcium Waves Occurs without Extracellular Calcium

(a)Calcium waves occurred in 20μM EGTA. Fertilized eggs were injected with 20nl of 0.5mM of Calcium Green-1 and after onset of first cleavage at the animal pole the eggs were observed from the vegetal side. Room temperature was about 26°C. 4x/0.13NA objective lens was used. The focal plane was adjusted to 400μm toward the vegetal pole from the equator of the egg. Confocal aperture was fully opened. Measurement was started at time 0 min. The original images were taken at 10 second intervals and each three succeeding images were averaged. The intensity of the fluorescence was shown in pseudo colors. Free calcium wave followed the cleavage furrow formation.

Note that at 23', the second wave is coming along the first cleavage furrow. At 25.5', the second cleavage furrow is coming to the equatorial region.

(b)The velocity of the calcium wave was calculated from the images shown in (a). The distance between the wave front and the edge of the egg was measured at each time point. Assuming that the wave occurred in the cortical region, the length of the path which the wave front had traveled was calculated and plotted as a function of time. The wave velocity was calculated as 2.8 μm/sec.

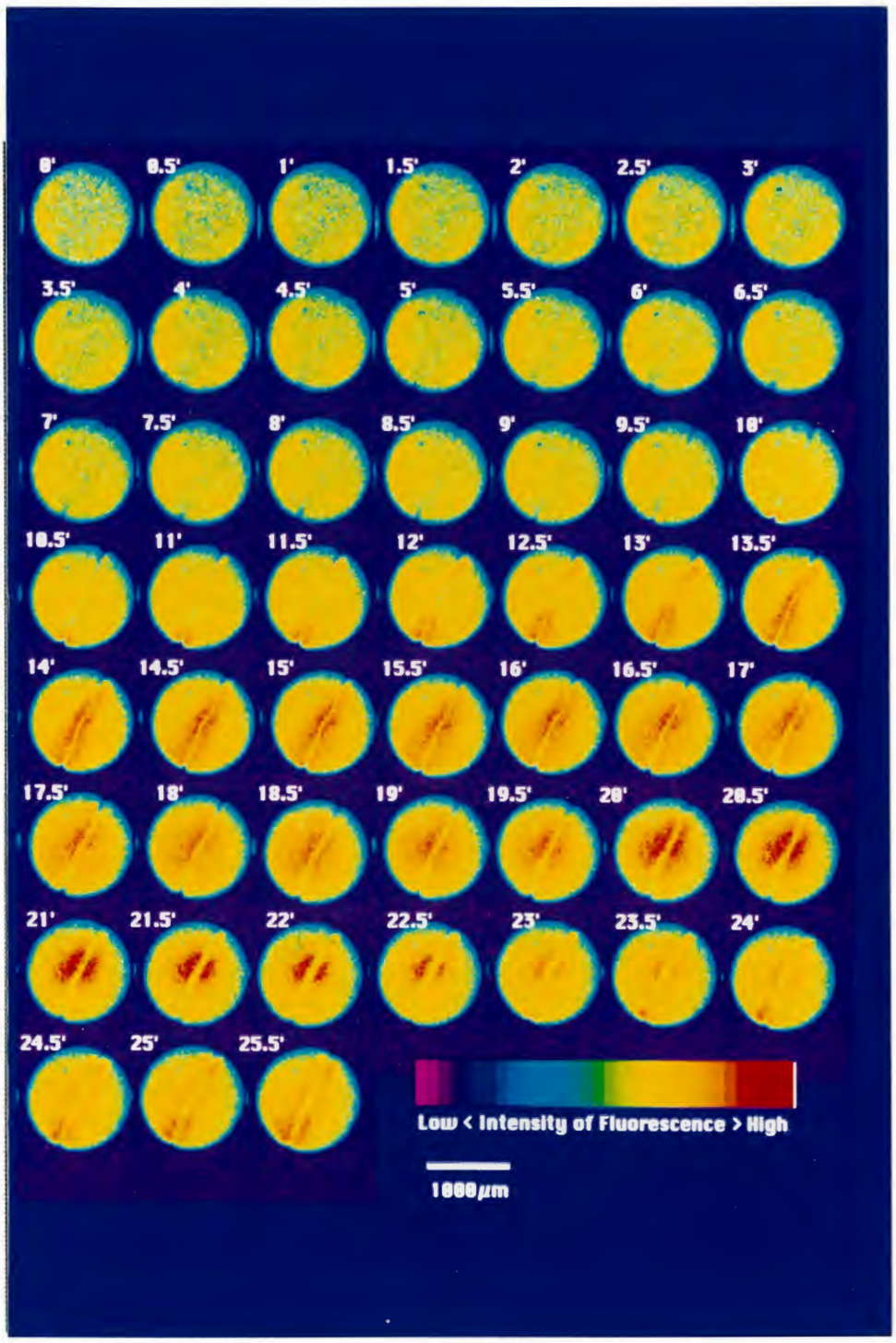
0'
0.5'
1'
1.5'
2'
2.5'
3'
3.5'
4'
4.5'
5'
5.5'
6'
6.5'
7'
7.5'
8'
8.5'
9'
9.5'
10'
10.5'
11'
11.5'
12'
12.5'
13'
13.5'
14'
14.5'
15'
15.5'
16'
16.5'
17'
17.5'
18'
18.5'
19'
19.5'
20'
20.5'
21'
21.5'
22'
22.5'
23'
23.5'
24'
24.5'
25'
25.5'
Low < Intensity of Fluorescence > High
1000μm

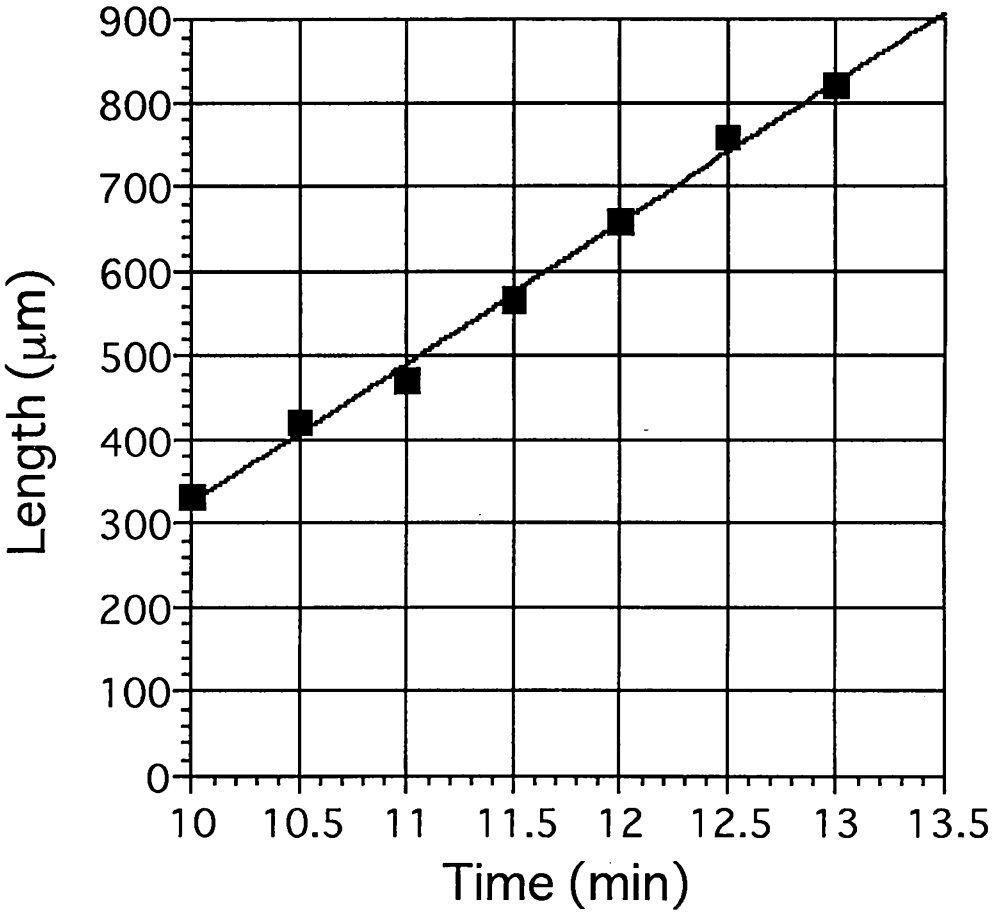
900
800
700
600
500
400
300
200
100
0
Length (μm)
10
10.5
11
11.5
12
12.5
13
13.5
Time (min)

Figure 5. Heparin Inhibits Calcium Waves

The measurements were carried out in 1/50 Steinberg's solution. The focal plane was determined to acquire maximum fluorescence over embryo. 4x/0.13NA objective lens was used. Room temperature was 25°C.

(a) Fluorescent images of heparin-injected/control embryos. In control embryo which was injected with 20 nl of 2 mg/ml De-N-sulfated heparin, free calcium waves were observed at the first cleavage furrow and the second cleavage furrow. In heparin-injected embryo, the rise at the first cleavage furrow was inhibited whereas the second cleavage has occurred. The onset of the first cleavage was delayed in heparin-injected embryos. The first cleavage furrow formation was also delayed as shown in the figure. The second cleavage could not complete normally and the embryo did not survive. Shown here are typical results. Five out of six experiments had the same results as shown here. Note that in the control embryo in Figure 5, the cleavage furrow was 'zipped' after calcium wave had passed as shown in Figure 3, while that of the heparin-injected embryo was not.

(b) Plot of fluorescence intensity in (a). Averaged fluorescence in the indicated region of embryo was plotted to show there was no significant rise through the experiment in heparin-injected embryo.


0'
3'
8'
13'
18'
23'
28'
33'
38'
43'
48'
Control Embryo
0'
3'
8'
13'
18'
23'
28'
33'
38'
43'
48'
1000μm
Heparin-Injected Embryo
Low
High

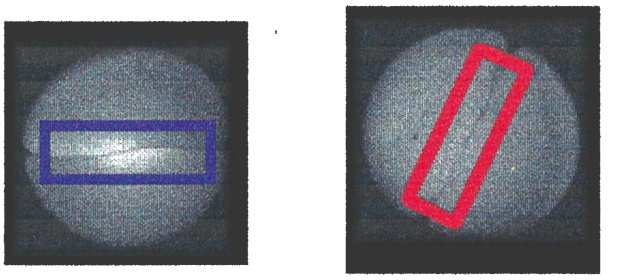

Control Embryo

Heparin-Injected Embryo

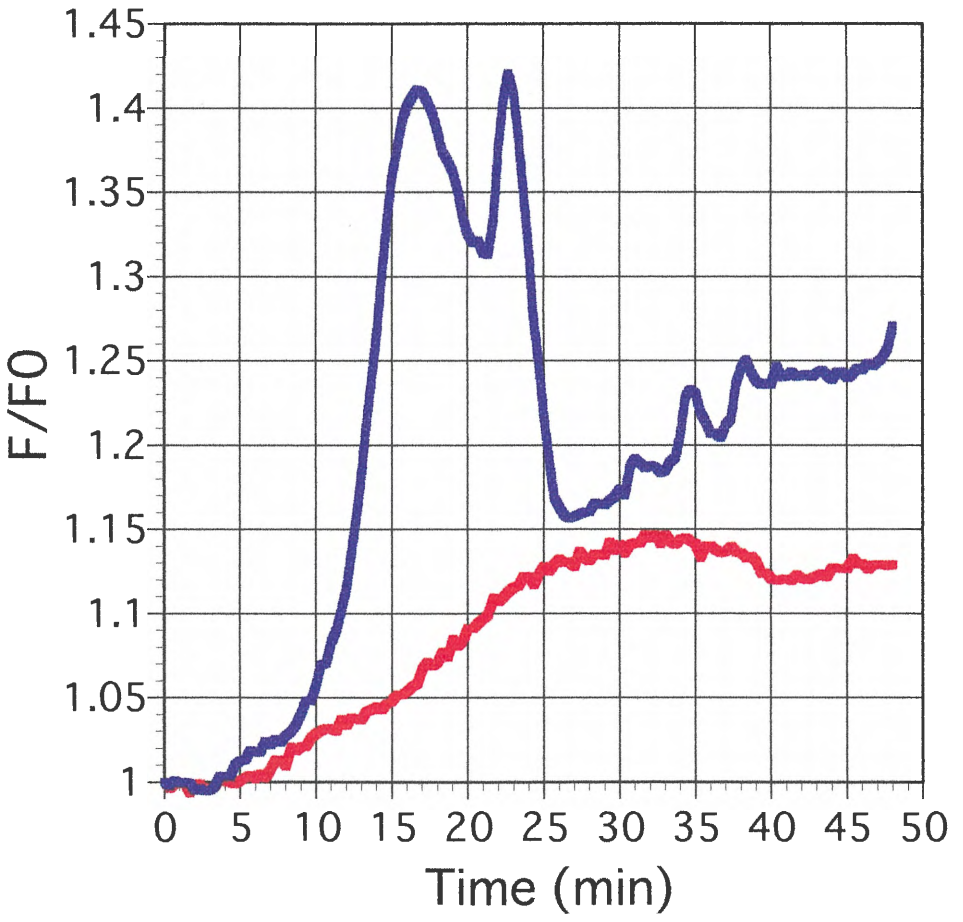

Figure 6. Oscillation of Fluorescence of Cleavage-Stage *Xenopus* Embryo

The embryos were injected with the calcium indicator dye, Calcium Green-1 after fertilization, transferred into Steinberg's solution and observed from the vegetal side with 4x/0.13NA objective lens. The focal plane was adjusted to 400μm toward the vegetal pole from the equator. The confocal aperture was set to fully opened condition. The averaged fluorescence intensity in the entire egg were plotted as F/F0, where F0 is the value at the start of the measurement. The intensity of the fluorescence oscillated with a period of 24.8 min. at 26°C. The images of the embryo at the timing of each peak are shown. Note that at the timing of each peak there are no free calcium rise associated with the cleavage furrow. The third cleavage of *Xenopus* egg takes place in the horizontal plane.

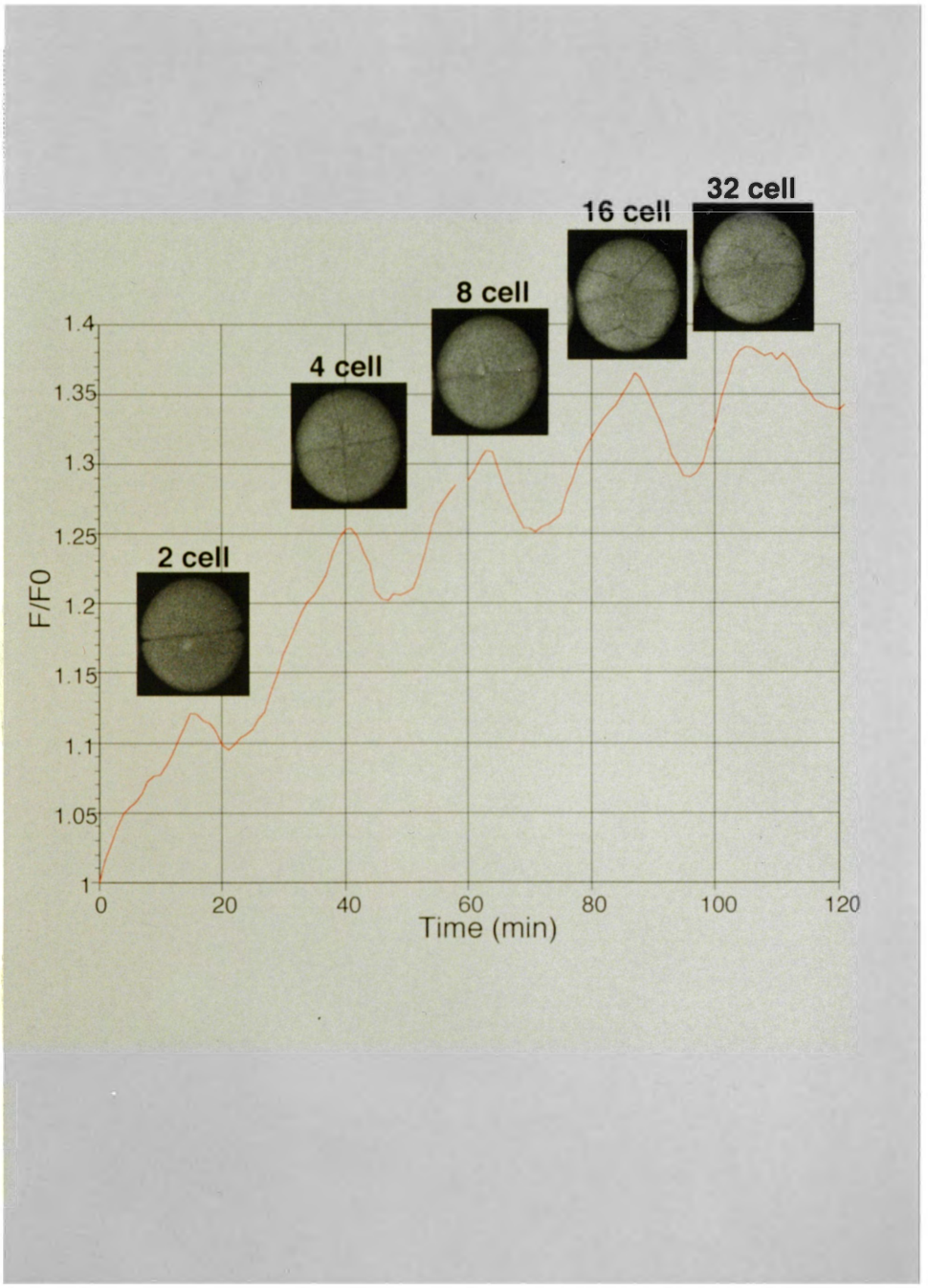
2 cell
4 cell
8 cell
16 cell
32 cell
F/F0
1.4
1.35
1.3
1.25
1.2
1.15
1.1
1.05
1
0
20
40
60
80
100
120
Time (min)

Figure 7. Oscillation of Fluorescence of Cleavage-Arrested Embryos

Fertilized eggs were injected with 20nl of 0.5mg/ml of colchicine and 0.5mM Calcium Green-1 and transferred into Steinberg's solution. The fluorescence intensity of colchicin-injected embryos oscillated with a periodicity of 40.1+/-3.3 min.(mean+/-SD, n=7) which was slightly longer than that of uninjected embryos(33.8+/-0.85min. (mean+/-SD, n=3)) at 24°C. Typical examples were shown here. The values of F/F0 were varied from egg to egg.

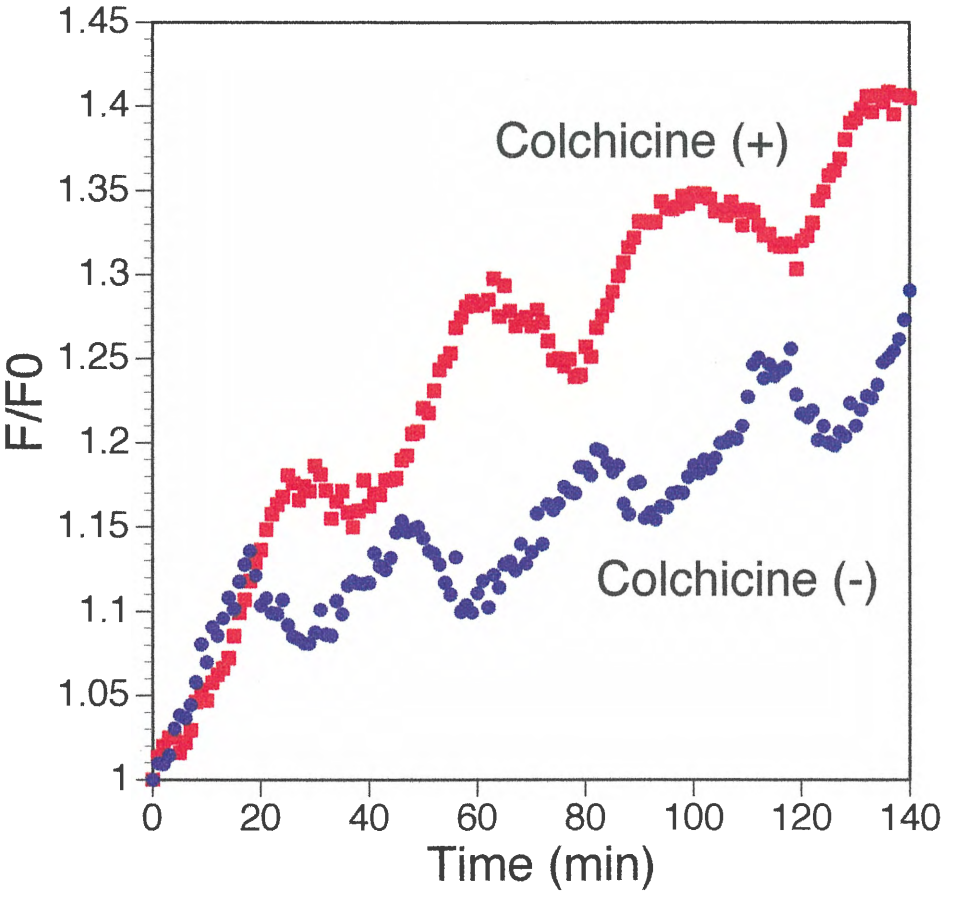
1.45
1.4
1.35
1.3
1.25
1.2
1.15
1.1
1.05
1
F/F0
Colchicine (+)
Colchicine (-)
0
20
40
60
80
100
120
140
Time (min)

Figure 8. Oscillation of Fluorescence Occurs in the Absence of Extracellular Calcium

Fertilized eggs were co-injected with 20nl of 0.5 mg/ml colchicine and 0.5 mM of Calcium Green-1. Calcium imaging was carried out in distilled water containing 50 μM of EGTA. All eggs observed (n=16) showed oscillatory changes of fluorescence. The period of the oscillation was 38.0+/-0.77 minutes (mean+/-SD, n=9) at 25°C. Typical one was shown here..

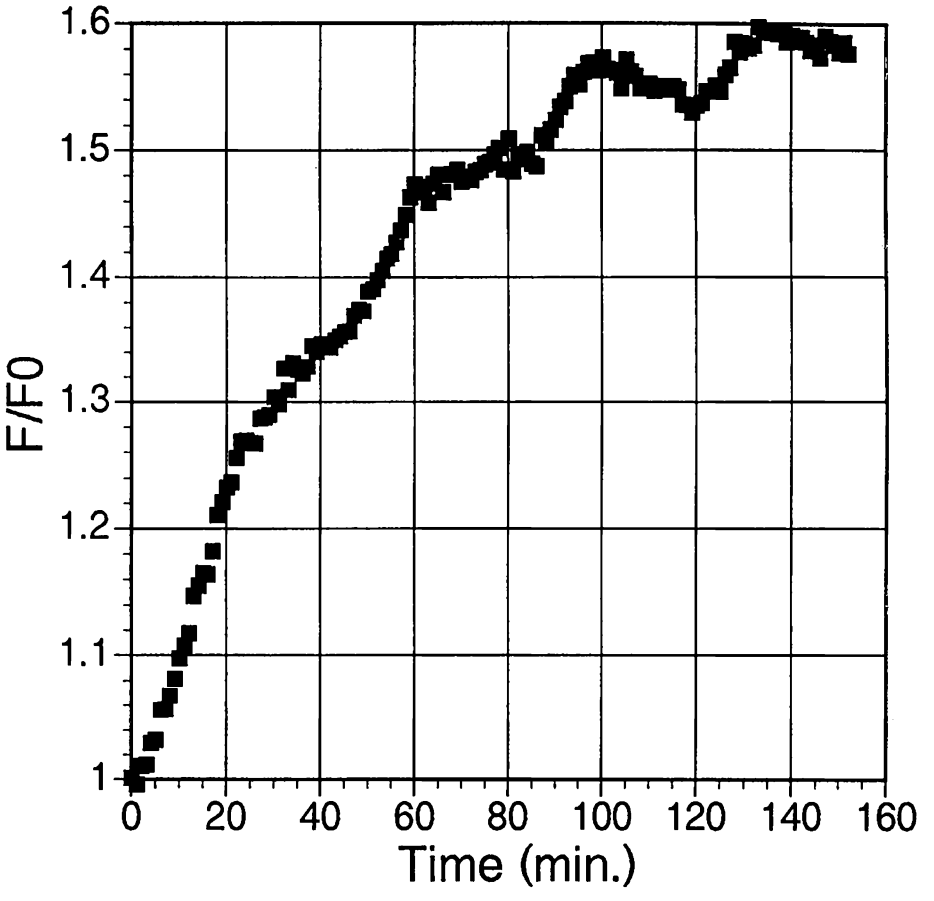
1.6
1.5
1.4
1.3
1.2
1.1
1
F/F0
0
20
40
60
80
100
120
140
160
Time (min.)

Figure 9. Heparin Inhibits the Oscillation

Fertilized eggs were injected with 20 nl of 2 mg/ml heparin or De-N-sulfated heparin (control), 0.5 mg/ml colchicine and 0.5 mM Calcium Green-1 and observed in Steinberg's solution. Control embryo (n=9) showed oscillatory changes of the fluorescence intensity with a period of 38.9+/-5.0 min. (mean/-SD, n=6) at 25°C. The period of the oscillation of the embryos injected with dye alone was 24.3+/-1.4 minutes (mean/-SD, n=3). The oscillation of the fluorescence intensity of heparin-injected embryos (n=9) was inhibited or significantly retarded. A typical result is shown here.

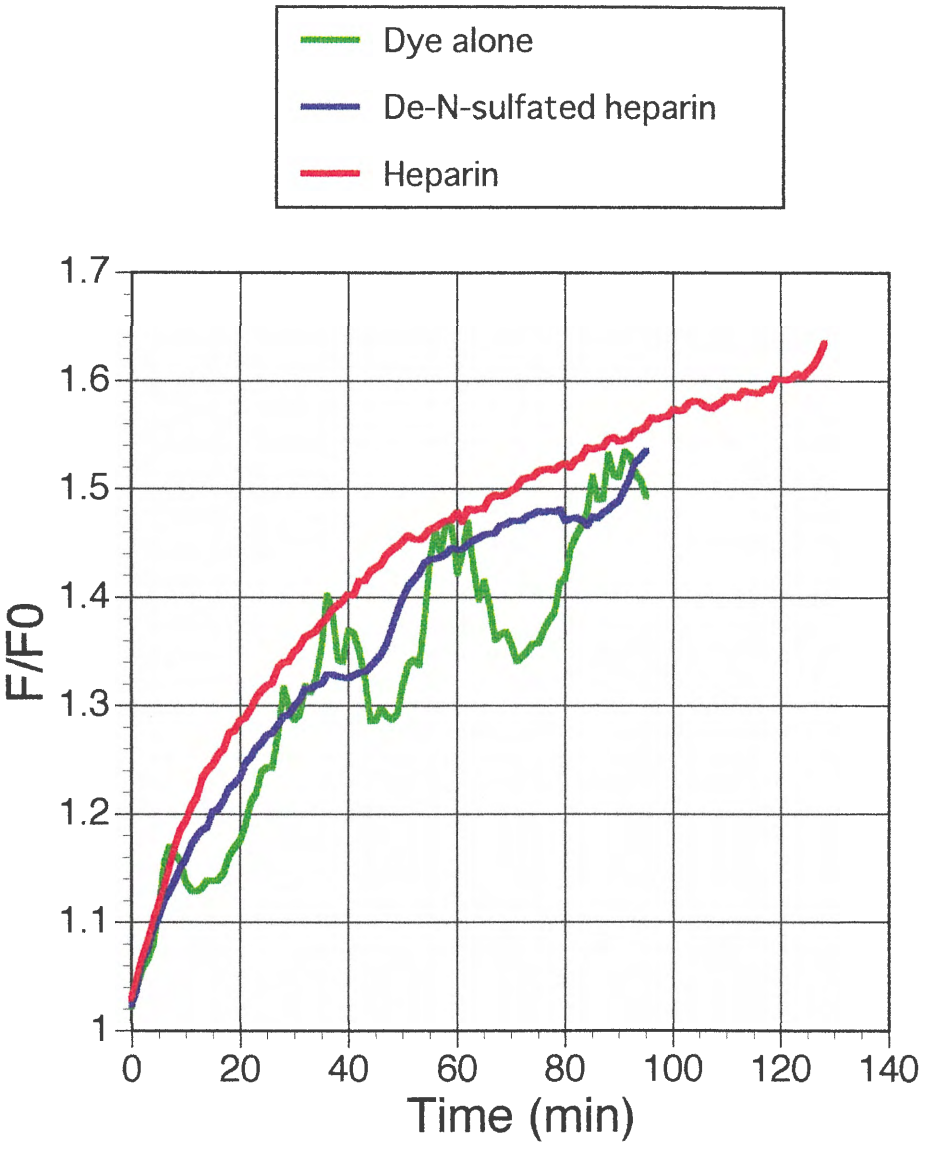
Dye alone
De-N-sulfated heparin
Heparin
F/F0
1.7
1.6
1.5
1.4
1.3
1.2
1.1
1
0
20
40
60
80
100
120
140
Time (min)

Figure 10. $InsP_3$-Induced Calcium Release from Microsomes of *Xenopus* Oocytes and Embryos

In order to measure the saturated level of calcium release, the measurement was carried out more than 7 minutes after $InsP_3$ addition. The radioactivity of calcium-45 remained in microsomes was counted. The amount of remained ^{45}Ca in microsomes in this time course was constant. The microsomes were prepared from *Xenopus* oocytes or 1-8 cell-stage embryos. Measurements were carried out at room temperature (25°C).

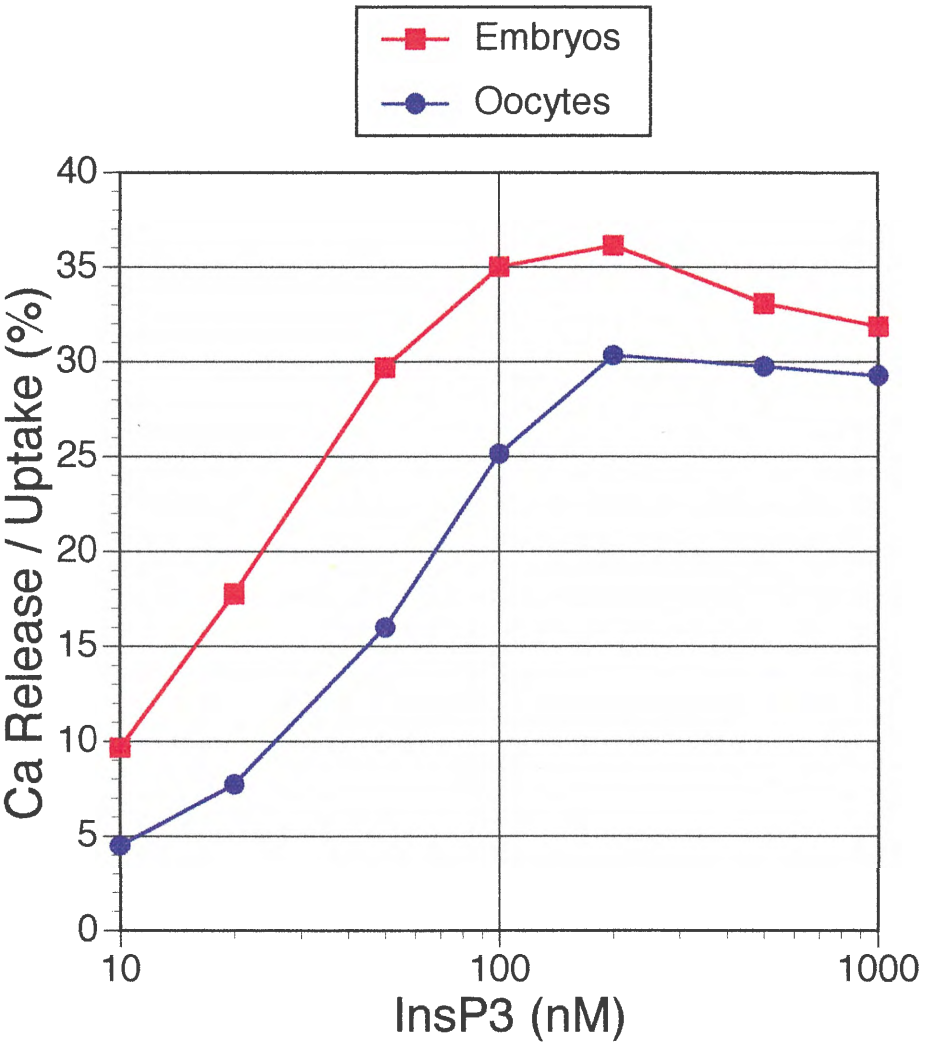
Embryos
Oocytes
Ca Release / Uptake (%)
0
5
10
15
20
25
30
35
40
10
100
1000
InsP3 (nM)

Figure 11. Effect of Heparin on IP_3 (100 nM)-Induced Calcium Release from Embryos Microsomes

Microsomes were prepared from 1-8 cell stage *Xenopus* embryos. After uptake of calcium into microsomes, heparin was added to the microsomes solution and incubated for 20 minutes. De-N-sulfated heparin was used in control experiment

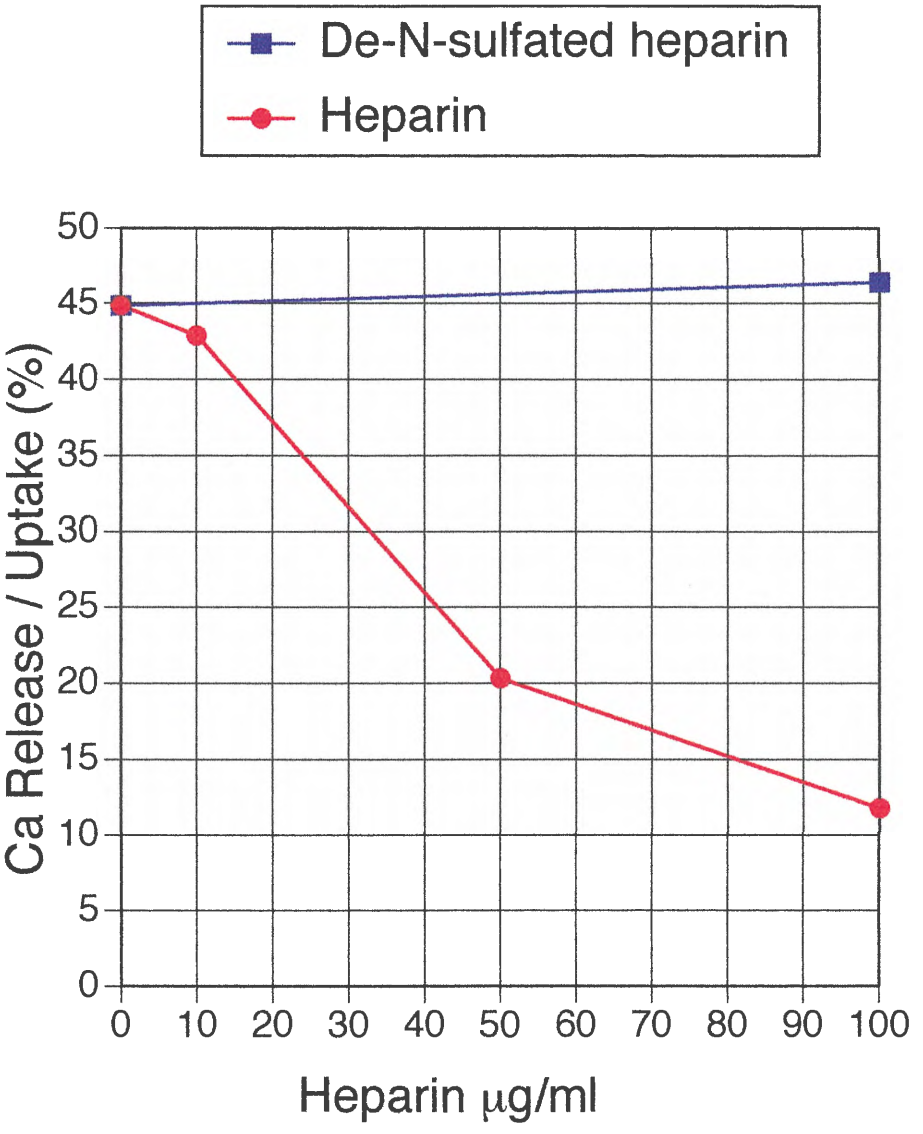
De-N-sulfated heparin
Heparin
Ca Release / Uptake (%)
50
45
40
35
30
25
20
15
10
5
0
0
10
20
30
40
50
60
70
80
90
100
Heparin μg/ml

Figure 12. Expression of $InsP_3$ Receptor Transcripts through *Xenopus* Development

Total RNA (20μg per lane) was analyzed by RNase protection for *Xenopus* $InsP_3$ receptor transcripts and subjected to 8M urea-5%PAGE.

.

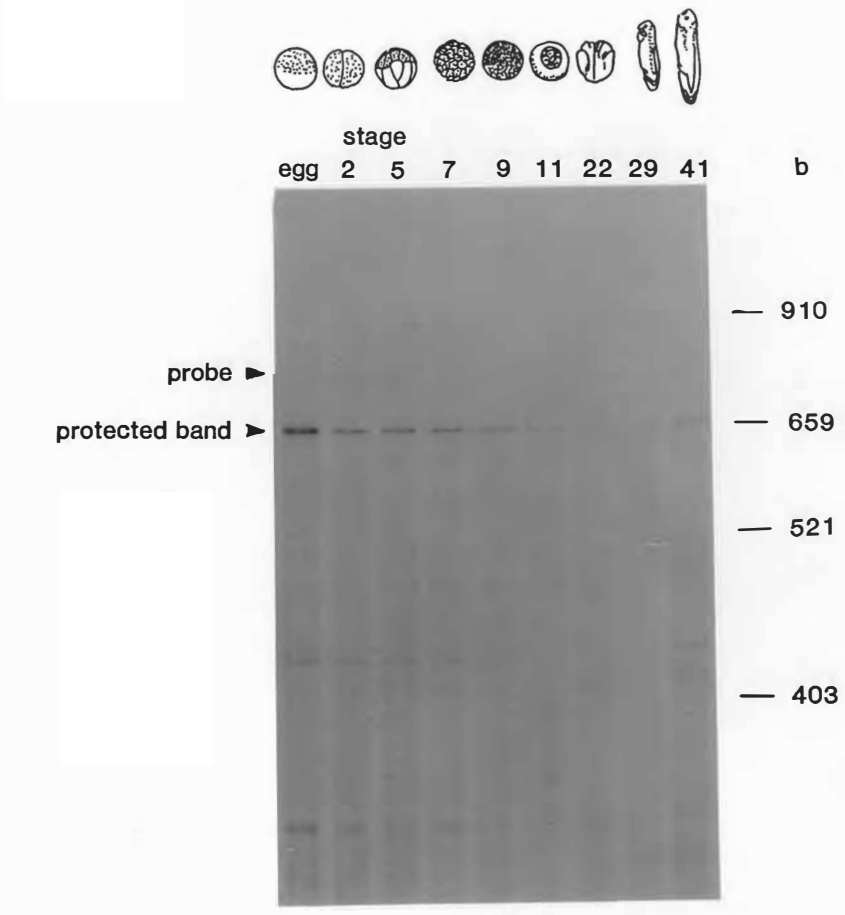
stage
egg 2 5 7 9 11 22 29 41
b
910
probe
protected band
659
521
403

Figure 13. Expression of InsP3 Receptor Proteins through *Xenopus* Development

Western bolt analysis using anti-GST-*Xenopus* InsP3 receptor.

Proteins of membrane fraction equivalent of one embryo was loaded at each lane.

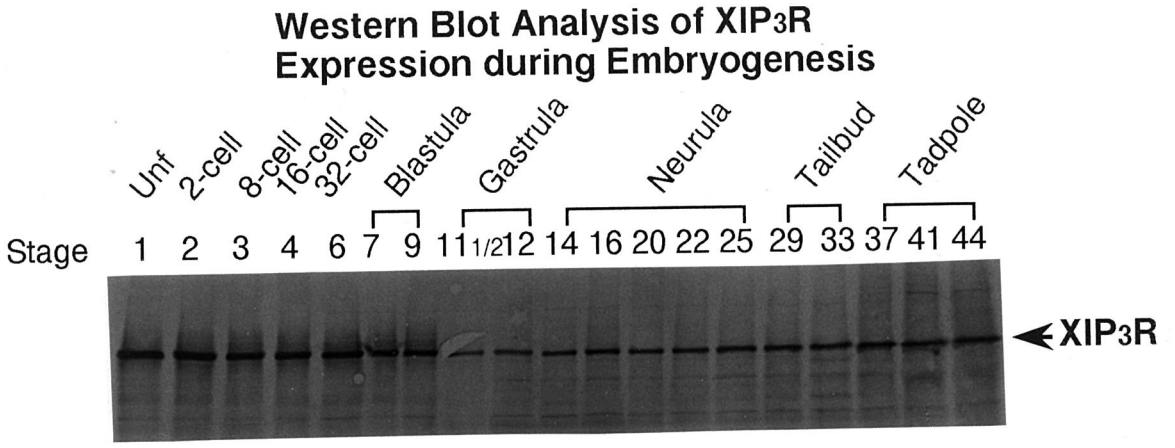
Western Blot Analysis of XIP3R
Expression during Embryogenesis
Unf
2-cell
8-cell
16-cell
32-cell
Blastula
Gastrula
Neurula
Tailbud
Tadpole
Stage 1 2 3 4 6 7 9 11 1/2 12 14 16 20 22 25 29 33 37 41 44
XIP3R

Figure 14. Subcellular Localization of InsP3 Receptor during Cell Cycle

Thirty two cell-stage embryos were fixed in 4%PFA and embedded in paraffin. The same section was double-stained with anti-GST-*Xenopus* $InsP_3$ receptor antiserum and anti-β-tublin antibody to show spindles at metaphase by indirect immunofluorescent microscopy. DNA was stained with DAPI.

(a-c) Metaphase. (a) DAPI staining. (b) $InsP_3$ receptors are rhodamine-labeled (red). (c) β-tublin was FITC-labeled to show the spindles.

(d-e)Anaphase. (d) DAPI staining. (e) $InsP_3$ receptors are FITC-labeled.

(f-g) Telophase. (f) DAPI stainging. (g) $InsP_3$ receptors are FITC-labeled. Only one divided nuclei is appeared in this section.

.

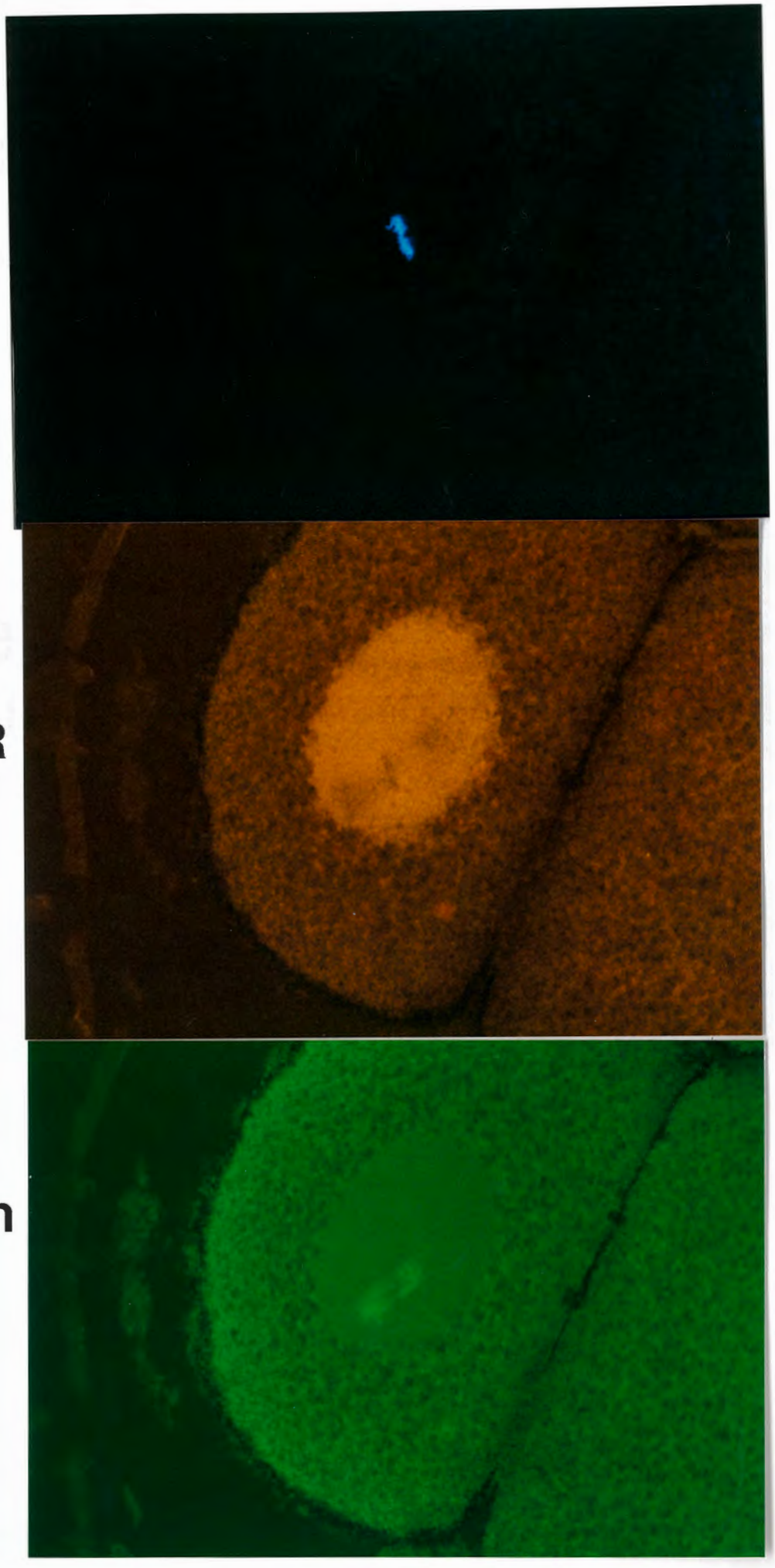
(a)
DNA
(b)
InsP3 R
(c)
β-Tublin
100μm

(d)

DNA

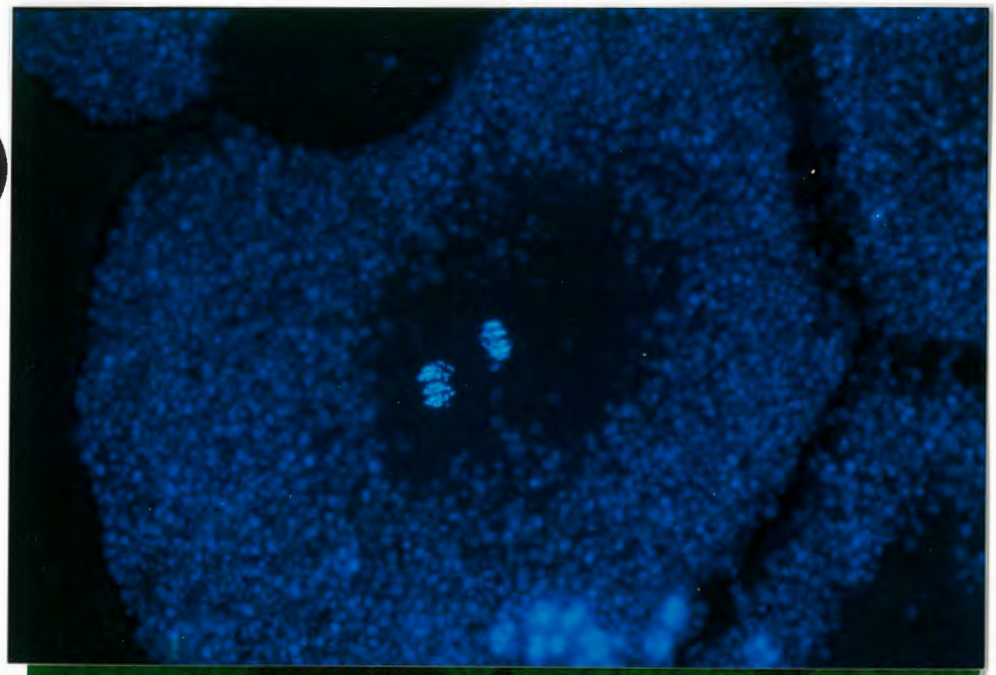

(e)

InsP3 R

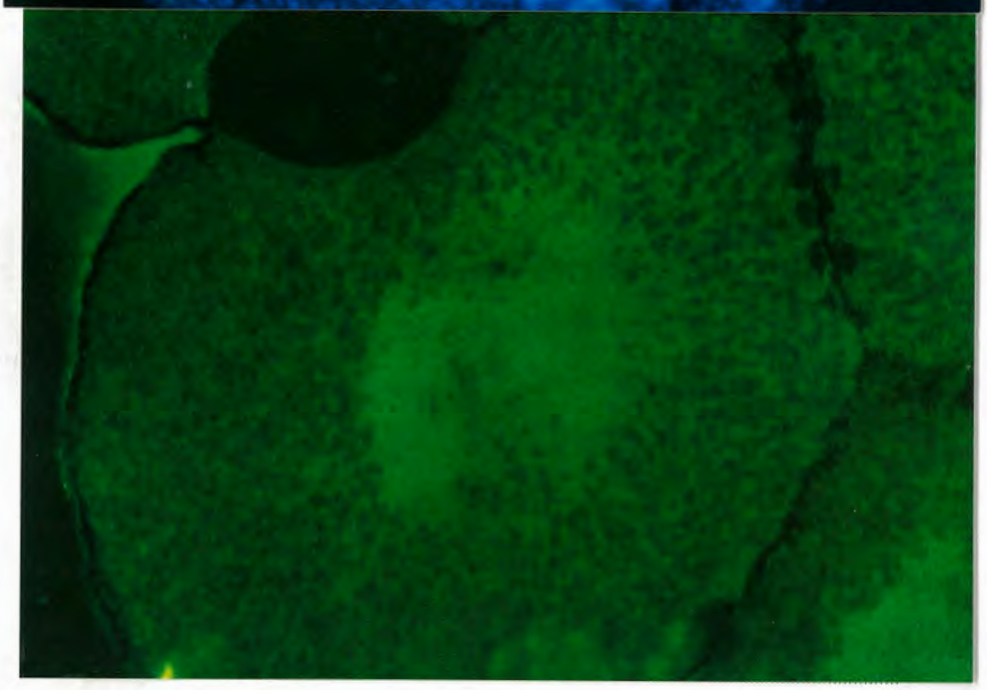

100μm

(f)
DNA

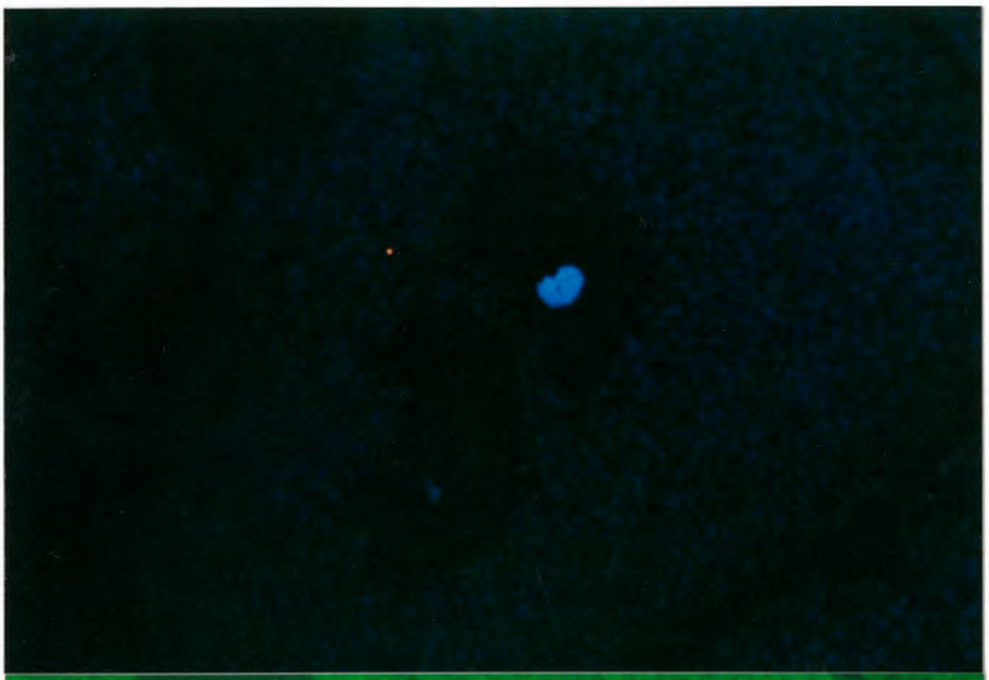

(g)
InsP3 R

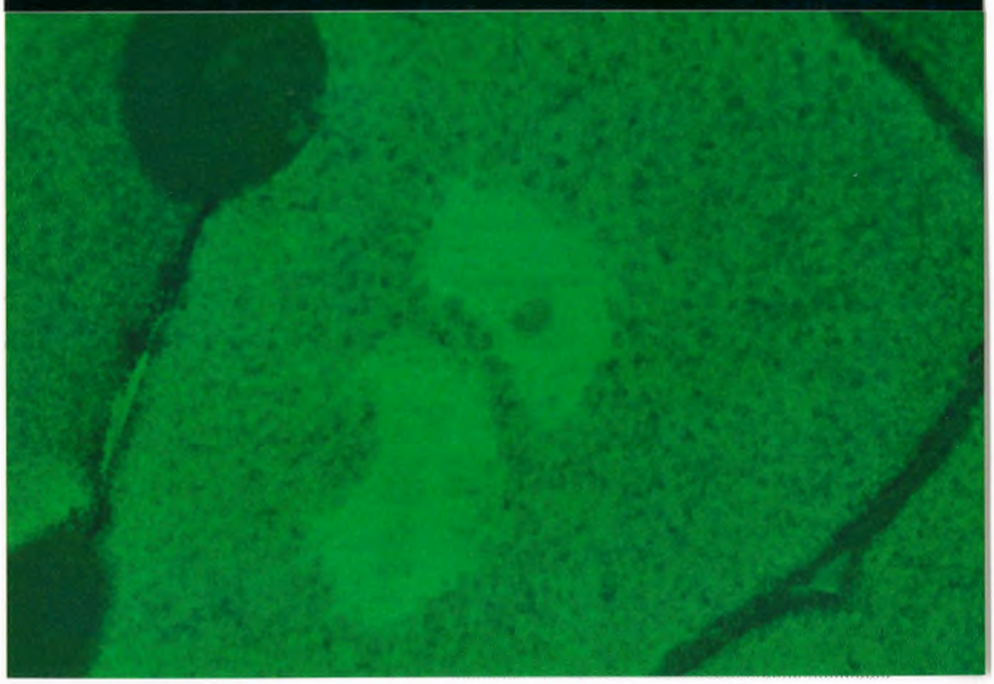

100μm

Figure 15. Immunolocalization of $InsP_3$ Receptors through Development

Immunocytochemistry using antiserum against $InsP_3$ receptor.

(a)32 cell-stage embryo.

(b)Blastula (St.8).

(c) Gastrula (St.11).

(d) Early neurula (St.16).

(e-i)Tailbud-stage embryo (St.24). (e) Sagital section. (f) Control staining using non-immune rabbit serum. (g-i) Coronal sections at indicated sites in (e).

(j-l)Tadpole (St.37/38). (j)Drawing of Tadpole (St.37/38) (from Nieuwkoop and Faber, 1967). (k) Sagital section. (h)Coronal section at the indicated sites in (j).

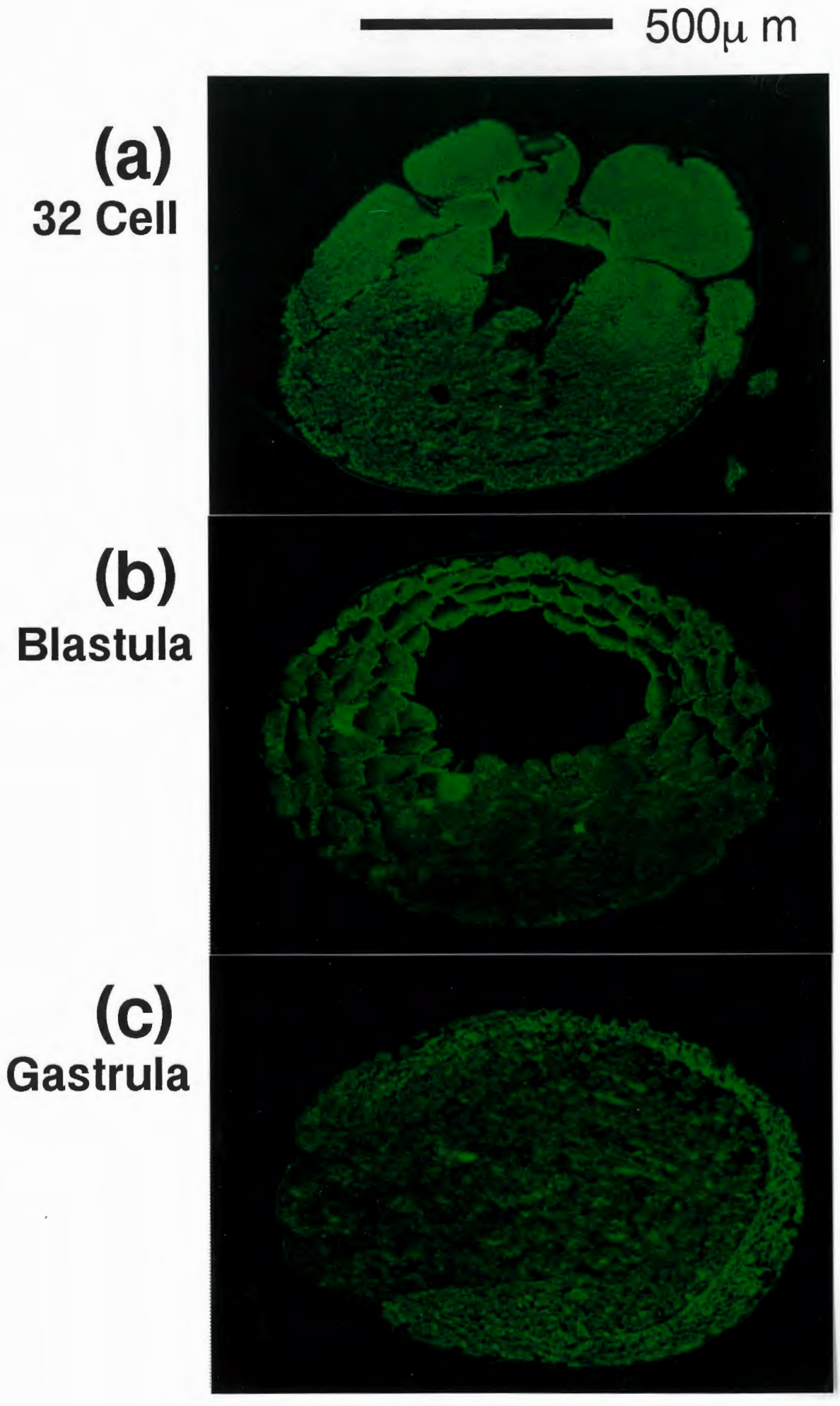
500μ m
(a)
32 Cell
(b)
Blastula
(c)
Gastrula

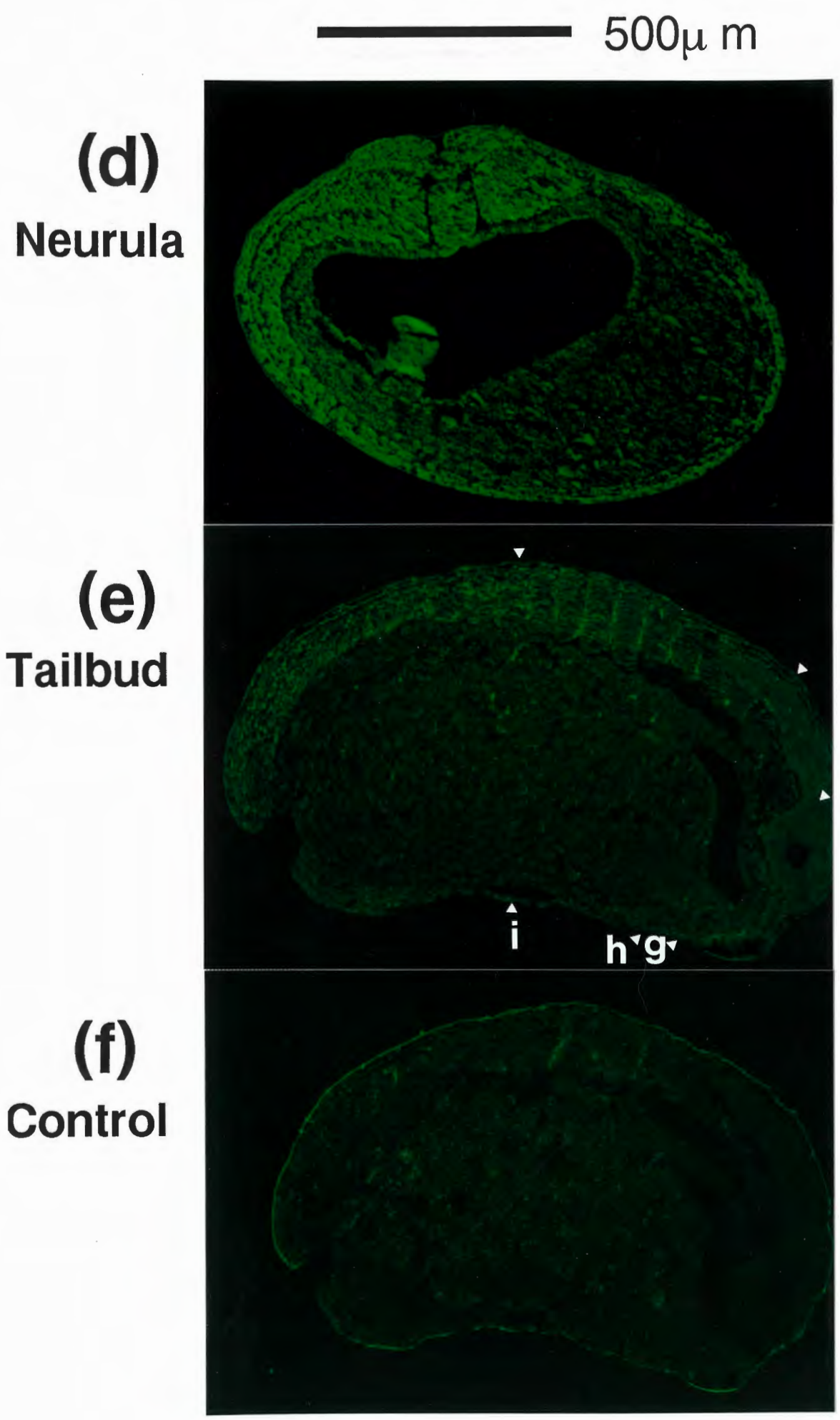
500μ m
(d)
Neurula
(e)
Tailbud
i
h
g
(f)
Control

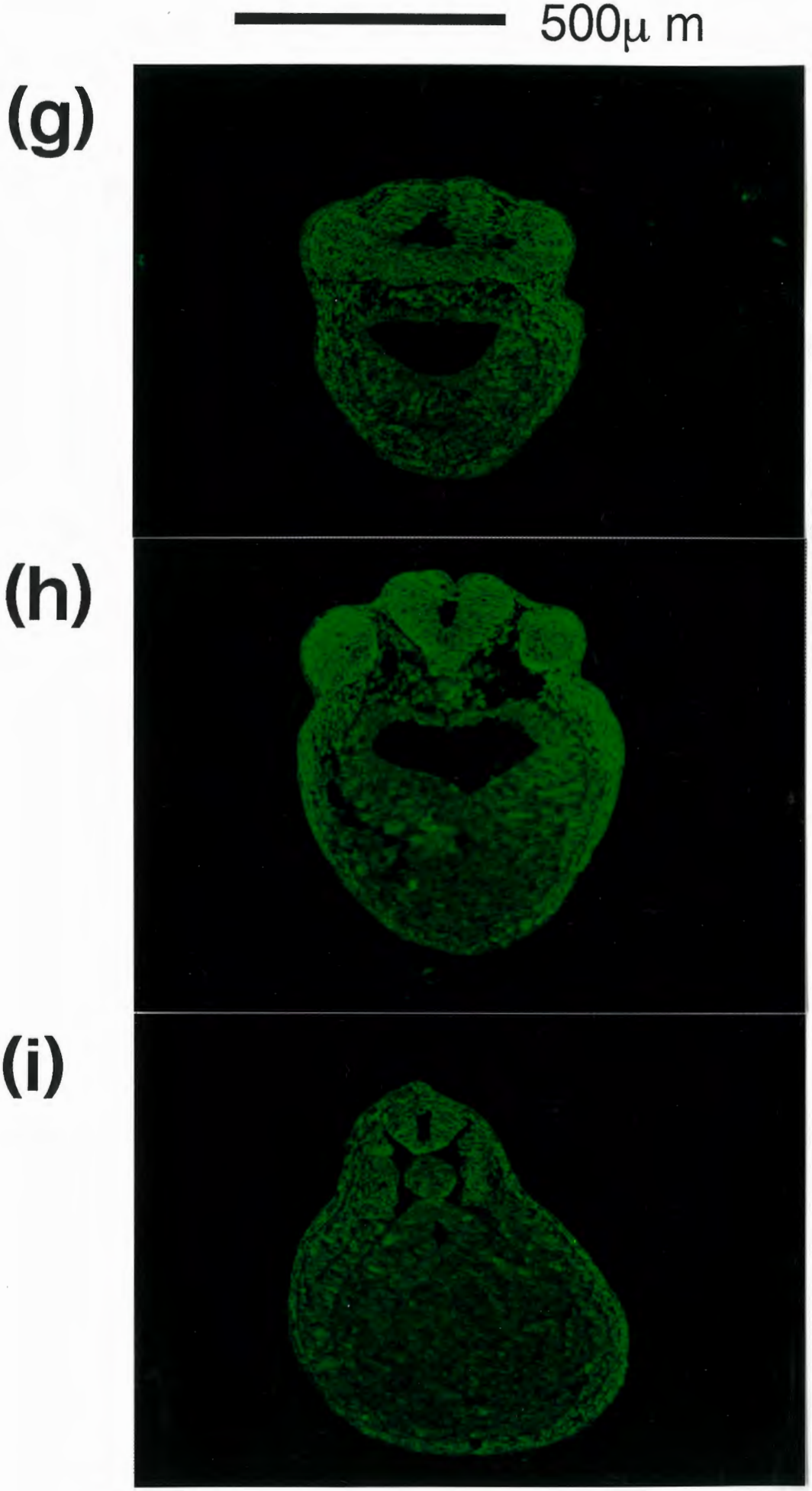
500μ m
(g)
(h)
(i)

(j)

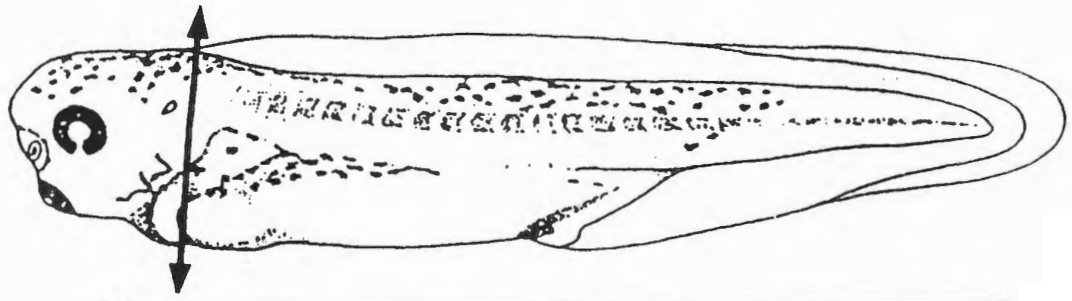

(k)
Tadpole

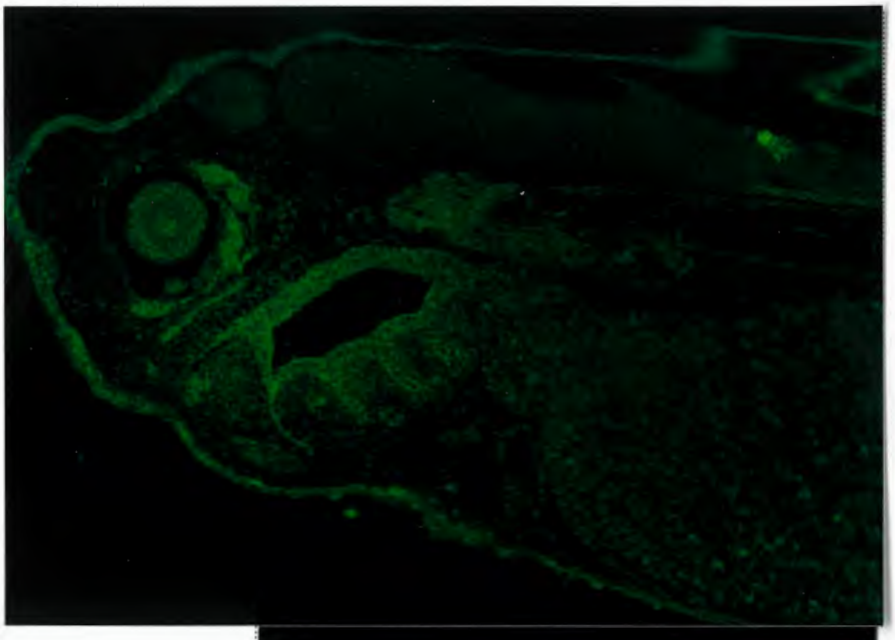

250μ m

(l)

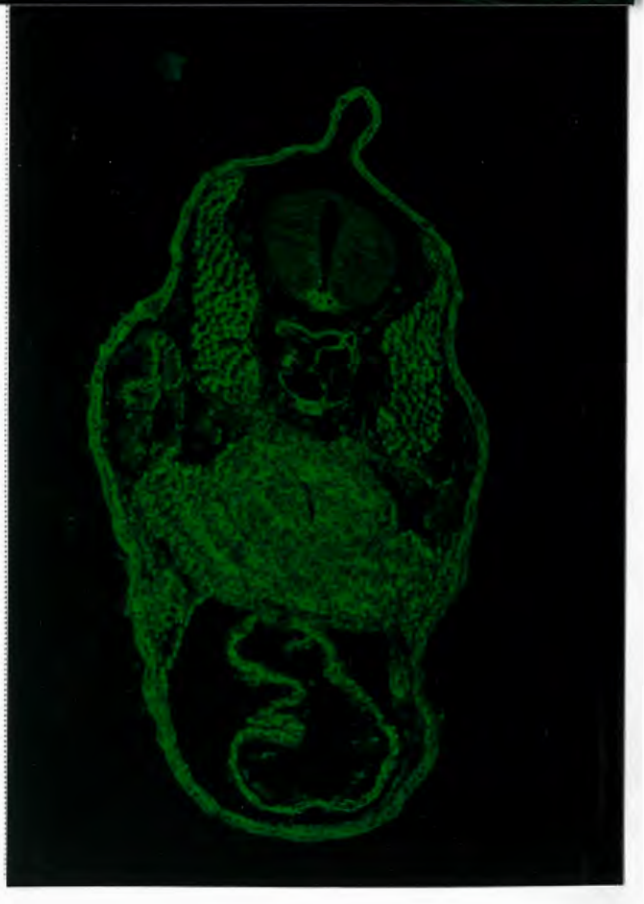

250μ m